PENNSTATE

1 8 5 5 *Department of Mechanical & Nuclear Engineering*

High-Pressure Combustion Chamber Dynamics

Vigor Yang
The Pennsylvania State University
University Park, Pennsylvania 16802, U.S.A.
**Email:* *vigor@psu.edu*

Presented at
International Symposium on Energy Conversion Fundamentals
Istanbul, Turkey, June 21-25, 2004

Report Documentation Page

Form Approved
OMB No. 0704-0188

1. REPORT DATE **22 JUN 2004**	2. REPORT TYPE **N/A**	3. DATES COVERED **-**

4. TITLE AND SUBTITLE **High-Pressure Combustion Chamber Dynamics**	5a. CONTRACT NUMBER 5b. GRANT NUMBER 5c. PROGRAM ELEMENT NUMBER
6. AUTHOR(S)	5d. PROJECT NUMBER 5e. TASK NUMBER 5f. WORK UNIT NUMBER
7. PERFORMING ORGANIZATION NAME(S) AND ADDRESS(ES) **The Pennsylvania State University University Park, Pennsylvania 16802, U.S.A.**	8. PERFORMING ORGANIZATION REPORT NUMBER
9. SPONSORING/MONITORING AGENCY NAME(S) AND ADDRESS(ES)	10. SPONSOR/MONITOR'S ACRONYM(S) 11. SPONSOR/MONITOR'S REPORT NUMBER(S)

12. DISTRIBUTION/AVAILABILITY STATEMENT
Approved for public release, distribution unlimited

13. SUPPLEMENTARY NOTES
See also ADM001793, International Symposium on Energy Conversion Fundamentals Held in Istanbul, Turkey on 21-25 June 2005., The original document contains color images.

14. ABSTRACT

15. SUBJECT TERMS

16. SECURITY CLASSIFICATION OF:			17. LIMITATION OF ABSTRACT	18. NUMBER OF PAGES	19a. NAME OF RESPONSIBLE PERSON
a. REPORT **unclassified**	b. ABSTRACT **unclassified**	c. THIS PAGE **unclassified**	**UU**	**51**	

Standard Form 298 (Rev. 8-98)
Prescribed by ANSI Std Z39-18

Why Supercritical Combustion Research?

Department of Mechanical & Nuclear Engineering

- most booster engines operate at supercritical conditions
- current understanding not sufficient to support design optimization

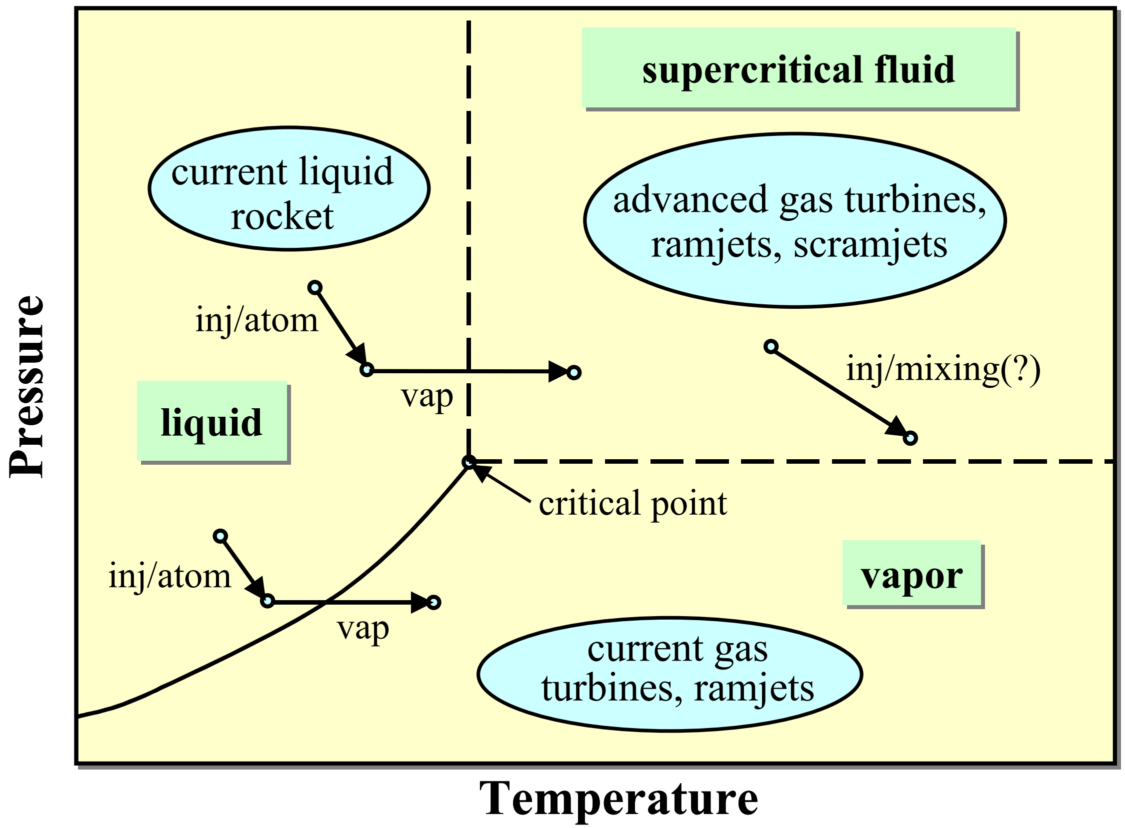

Liquid Rocket Chamber Conditions

Department of Mechanical & Nuclear Engineering

Critical Properties of Propellants

	Pcr (MPa)	Tcr (K)
H_2	1.3	33.3
Oxygen	5.04	154.4
RP-1	2.344	685.95

F-1 Engine (Saturn V)

	Fuel Inj.	Oxy Inj.	Cham.
T (K)	294.3	89.5	3546
P (MPa)	7.9	8.8	7.8

Space Shuttle Main Engine

	Fuel Inj.	Oxy Inj.	Cham.
T (K)	879.0	126.0	3700
P (MPa)	24.8	33.0	22.58

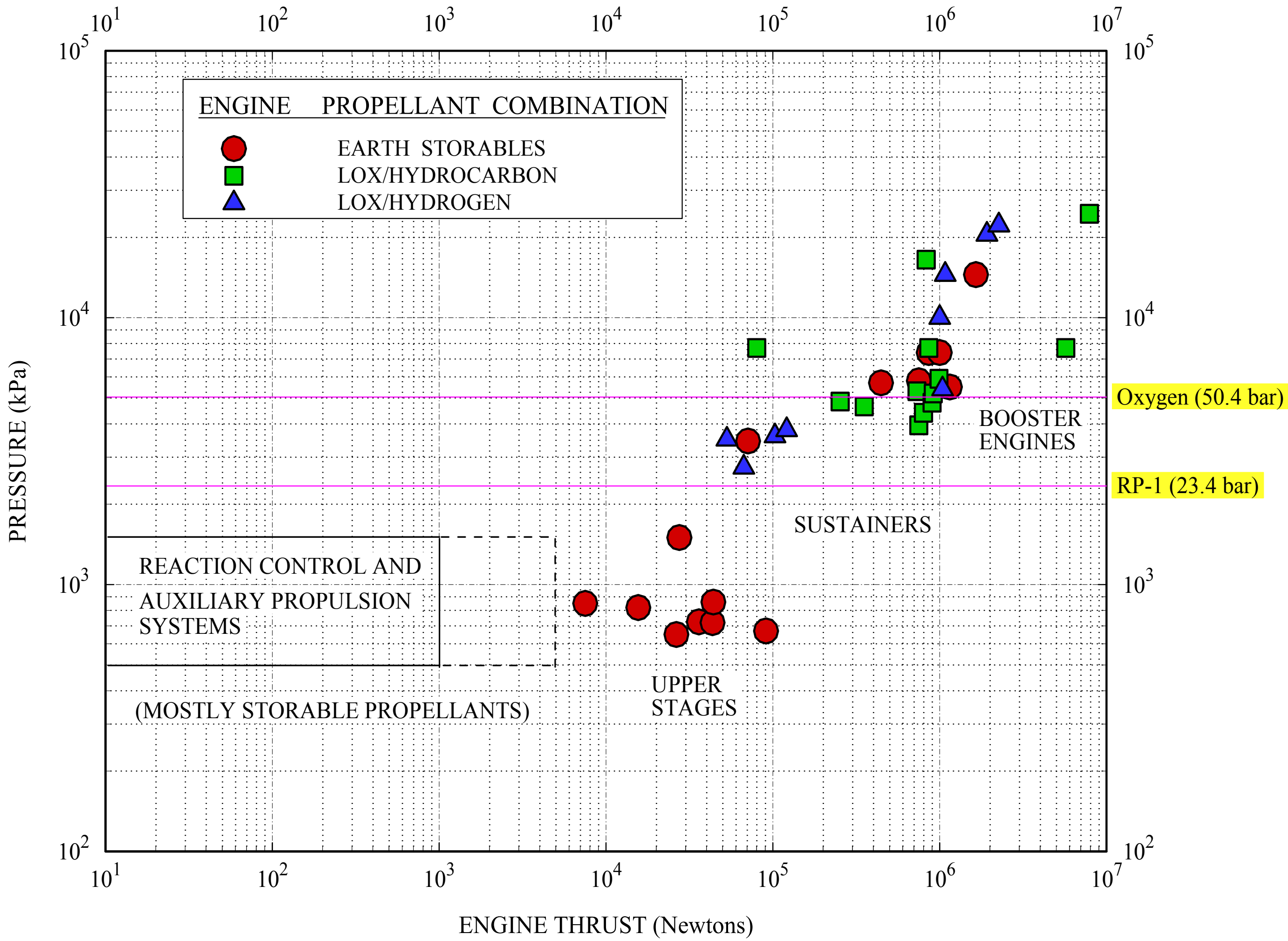

Flow Diagram of RD-170 Engine

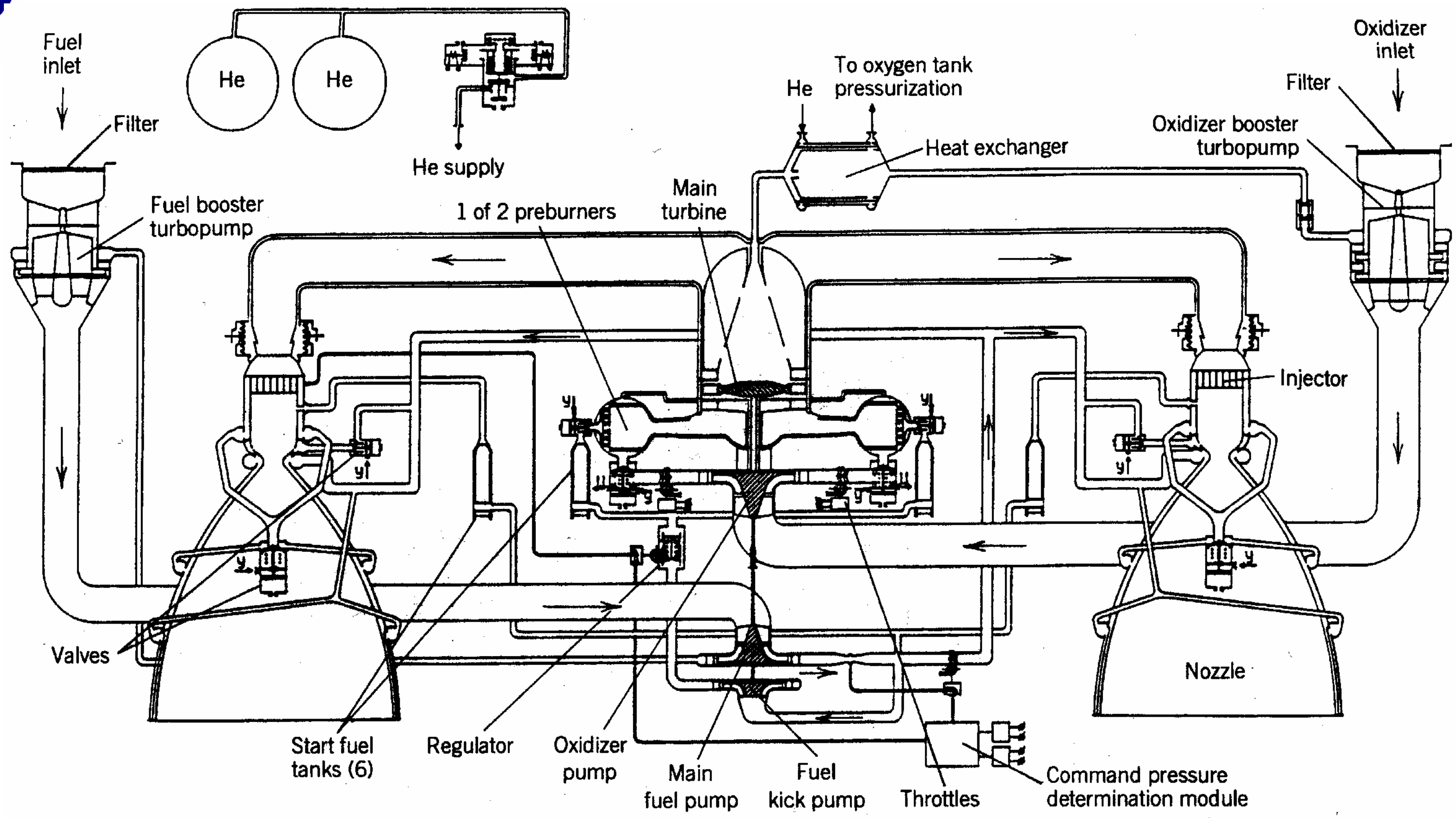

– Energia booster and Zenit first stage, up to 10 flights.
– LOX/kerosene, one main two boost turbopumps
– 806 ton thrust (vacuum), 337 seconds of I_{sp}, O/F ratio of 2.63
– Chamber pressure 250 bar, turbine inlet pressure 519 bar and temperature 772 K

Worldwide Efforts on Supercritical Combustion Research (1/2)

- Tamura et al. / NAL (Japan)
- Mayer, Oschwald, Haidn, etc. / DLR (Germany)
- Habiballah,Vingert, Grisch, etc. / ONERA (France)
  Candel et al. / Ecole Central Paris (France)
- Woodward, Pal, Santoro, etc. / Penn State (USA)
  Talley, Chehroudi, etc. / AFRL (USA)
  Blevins, Morris, etc. / NASA Marshall (USA)

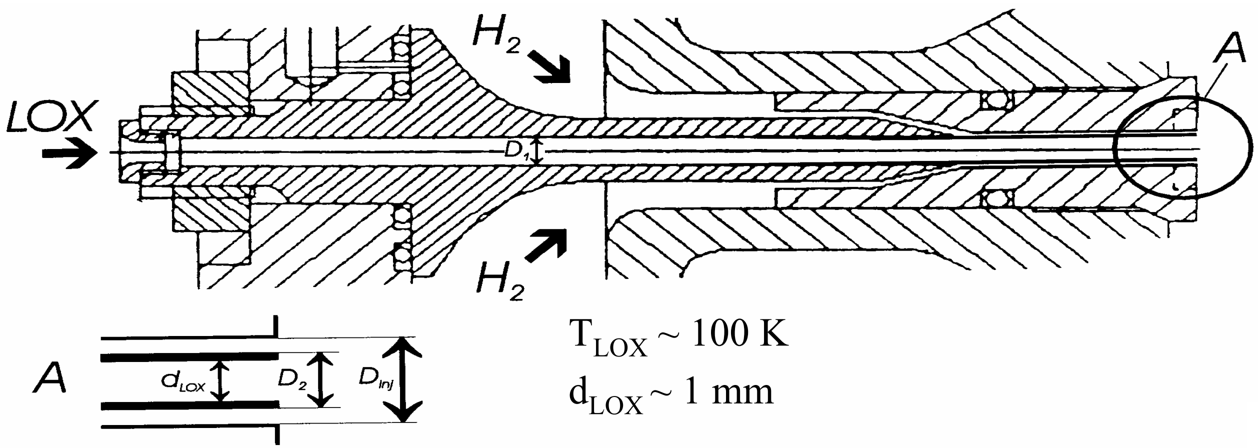

T_{LOX} ~ 100 K
d_{LOX} ~ 1 mm

Worldwide Efforts on Supercritical Combustion Research (2/2)

droplet → **spray** → **injector element** → **full-scale engine**

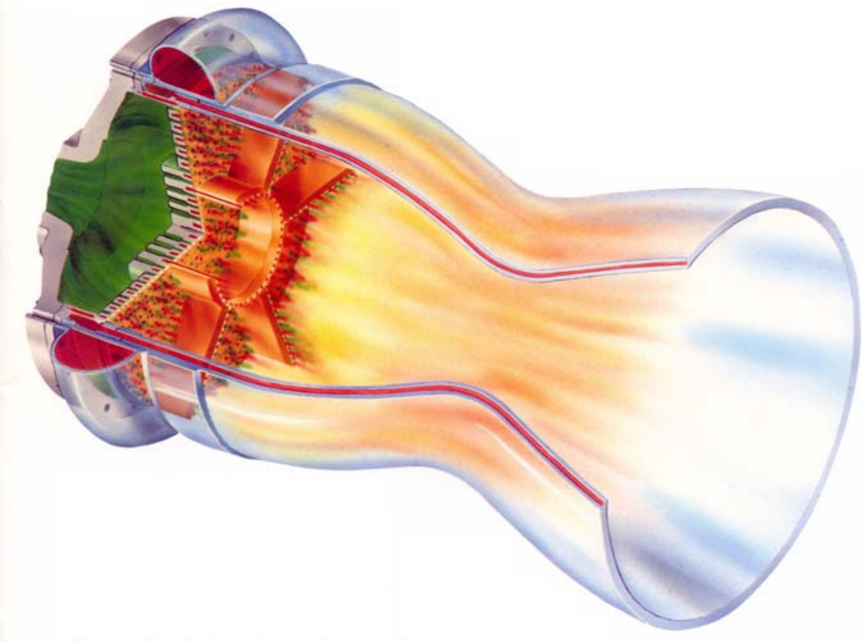

- Oefelein / DoE Sandia Lab. (USA)
- Bellan / NASA JPL (USA)
- Farmer / U. of Nevada (USA)
- Habiballah, et al. / ONERA (France)
- Yang / Penn State (USA)

Shadowgraph Results – LN2 into GN2

Chehroudi et. al., AIAA 99-0206, AIAA 99-2489

$p_{cr} = 3.39$ MPa, $T_{cr} = 126$ K, $T_{\infty} = 300$ K, $T_{in} = 99 \sim 120$ K

$u_{in} = 10 \sim 15$ m/s, $D_{in} = 0.254$ mm, $Re = 25{,}000 \sim 75{,}000$

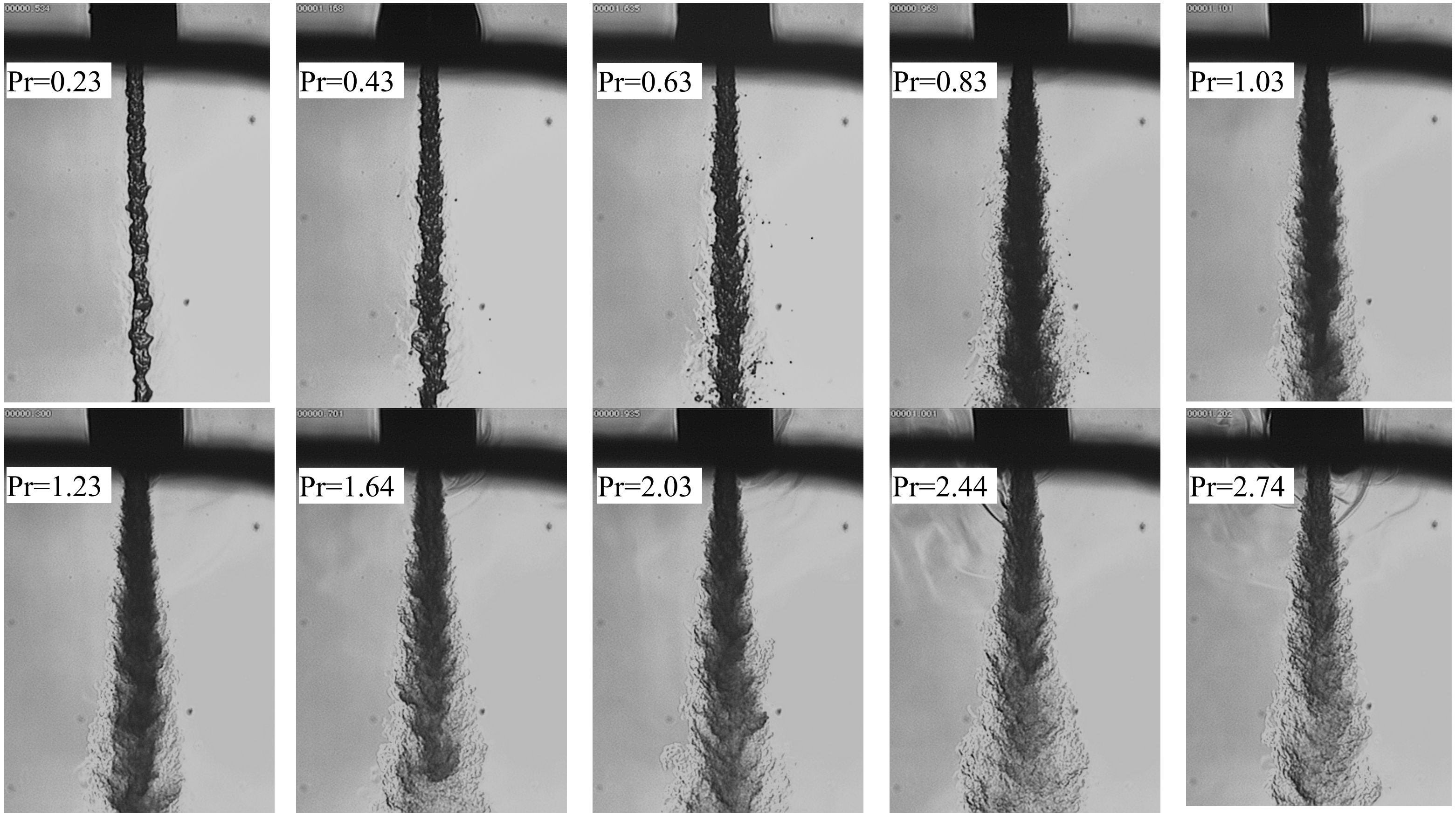

PENNSTATE
1 8 5 5

Characteristics of Supercritical Fluid Jet

Department of Mechanical & Nuclear Engineering

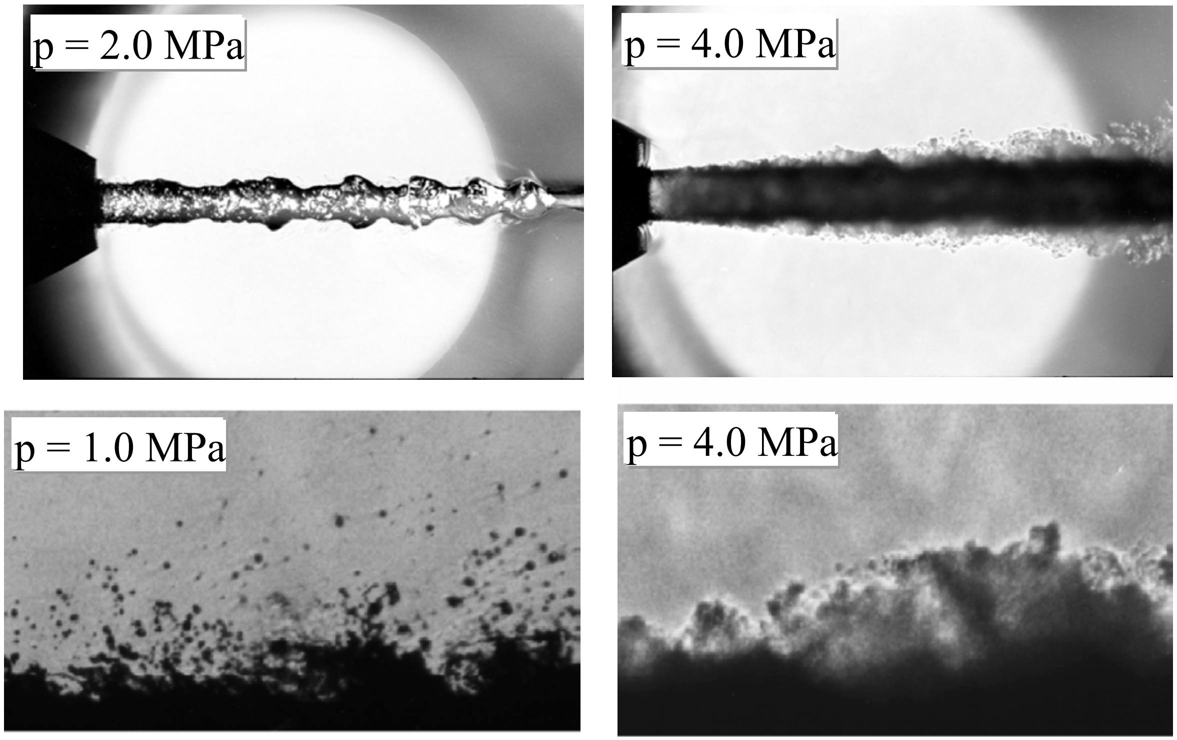

Mayer et al.
AIAA 1996-2620
T_{LN2} = 105 K
T_{GN2} = 300 K
u_{LN2} = 10 m/s
D_{in} = 1.9 mm

- **Thermodynamic non-idealities and transport anomalies in transcritical regime**
  - rapid property variations   - large density gradient
- **Diminishment of surface tension and enthalpy of vaporization**
- **Pressure-dependent solubility**
- **High Reynolds number**

Effect of Pressure on Turbulence Scales

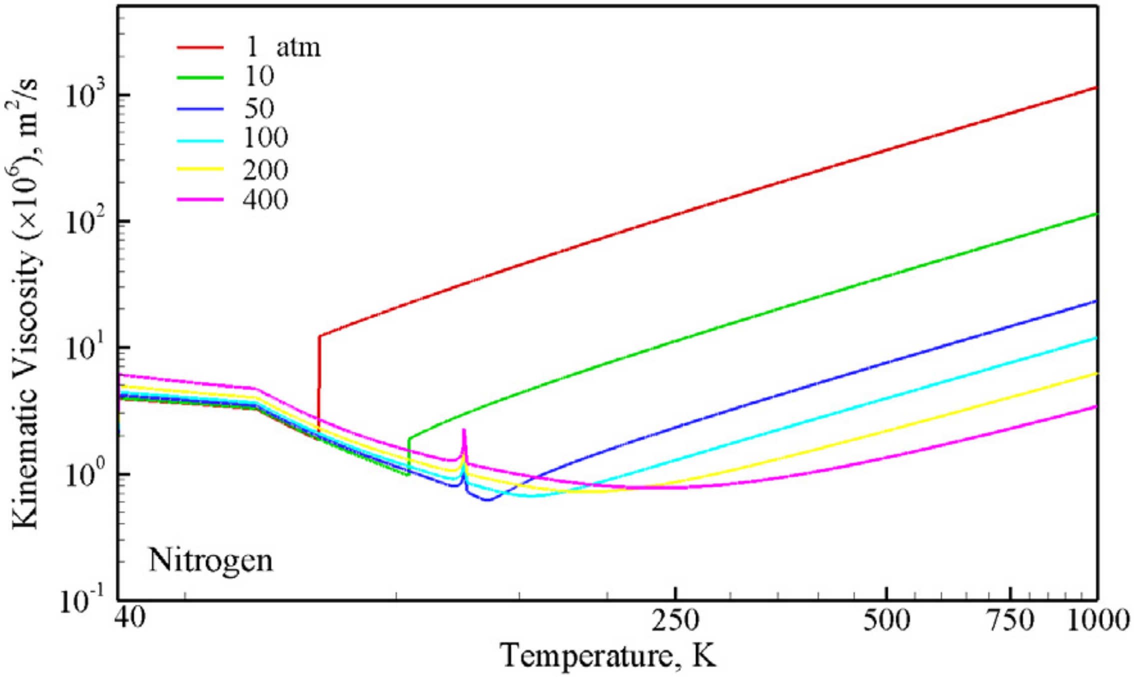

- Pressure increases from 1 to 10^2 atm, Re_t increases by 10^2
- Kolmogorov microscale $\eta_t/l_t \sim Re_t^{-3/4}$ (decrease by 1.5 order)
- Taylor microscale $\lambda_t/l_t \sim Re_t^{-1/2}$ (decrease by 1.0 order)

PENNSTATE

1 8 5 5

LES Formulation of Supercritical Fluid Dynamics

Department of Mechanical & Nuclear Engineering

• Favre-filtered conservation equations

$$\frac{\partial \bar{\rho}}{\partial t} + \frac{\partial (\bar{\rho} \tilde{u})}{\partial x_j} = 0$$

$$\frac{\partial(\bar{\rho}\tilde{u}_j)}{\partial t} + \frac{\partial(\bar{\rho}\tilde{u}_i\tilde{u}_j + \bar{p}\delta_{ij} - \bar{\tau}_{ij})}{\partial x_j} = -\frac{\partial(R_{ij} + L_{ij} + C_{ij})}{\partial x_j}$$

$$\frac{\partial(\bar{\rho}\tilde{E} + q)}{\partial t} + \frac{\partial[(\bar{\rho}\tilde{E} + \bar{P})\tilde{u}_j - \overline{u_i\tau_{ij}}]}{\partial x_j} = -\frac{\partial(K_j + Q_J + q_j)}{\partial x_j}$$

• Closure requirements

- Thermodynamic and transport properties $Z, C_p, \mu, \lambda, D_{im}$
- Subgrid-scale turbulence interaction $R, \quad L, \quad C$
- Chemical kinetics $\bar{\dot{\omega}}_i$

Equations of State

- Soave-Redlich-Kwong (SRK)

$$p = \frac{RT}{v-b} - \frac{a}{v(v+b)}$$

- Peng-Rubinson (PR)

$$p = \frac{RT}{v-b} - \frac{a}{v(v+b)+b(v-b)}$$

- Benedict-Webb-Rubin (BWR)

$$p = \sum_{n=1}^{9} a_n \rho^n + \sum_{n=10}^{15} a_n \rho^{2n-17} e^{-\gamma\rho^2}$$

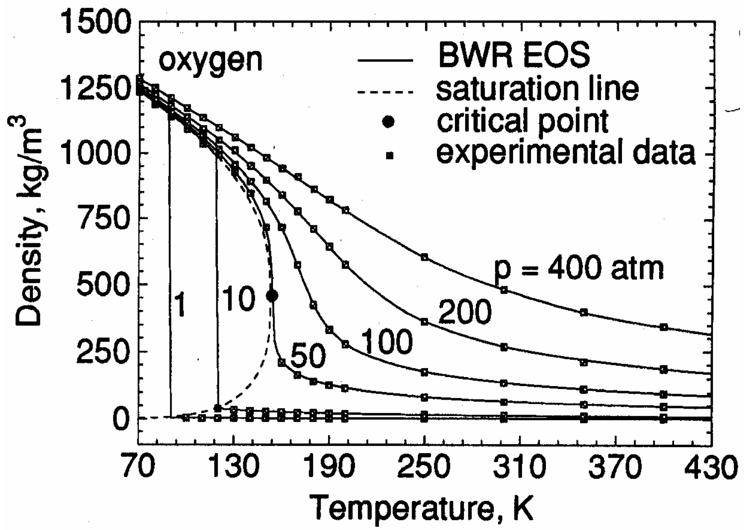

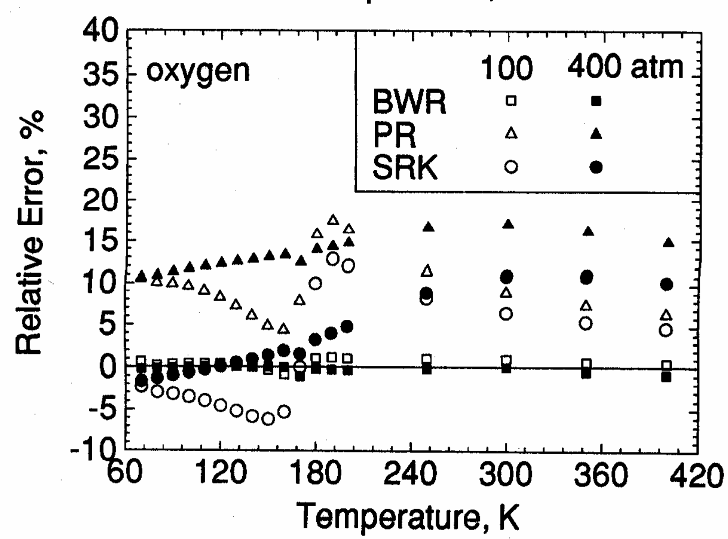

Evaluation of Thermodynamic Properties

- Sensible enthalpy: $h(\rho,T) = h^0(T) + \Delta h_{exc}(\rho,T)$
- Internal energy: $u(\rho,T) = u^0(T) + \Delta u_{exc}(\rho,T)$
- Specific heat $C_p(\rho,T) = C_p{}^0(T) + \Delta C_{p,exc}(\rho,T)$

$\Delta h_{exc}, \Delta u_{exc}, \Delta C_{p,exc}$ = dense fluid corrections

$h^0(T), u^0(T), C_p^0(T),$ = values in dilute-gas limit

Pressure-explicit type of EOS:

$$\Delta h_{exc} = \int_0^\rho \left[\frac{p}{\rho^2} - \frac{T}{\rho^2}\left(\frac{\partial p}{\partial T}\right)_\rho \right] d\rho + RT(Z-1)$$

$$\Delta u_{exc} = \int_0^\rho \left[\frac{p}{\rho^2} - \frac{T}{\rho^2}\left(\frac{\partial p}{\partial T}\right)_\rho \right] d\rho$$

$$\Delta C_{p,exc} = -T\int_0^\rho \left[\frac{1}{\rho^2}\left(\frac{\partial^2 p}{\partial T^2}\right) d\rho + \frac{T(\partial p/\partial T)_\rho^2}{\rho^2(\partial p/\partial \rho)_T} \right] - R$$

PENNSTATE
1855

Thermophysical Properties of Nitrogen

Department of Mechanical & Nuclear Engineering

- compressibility factor

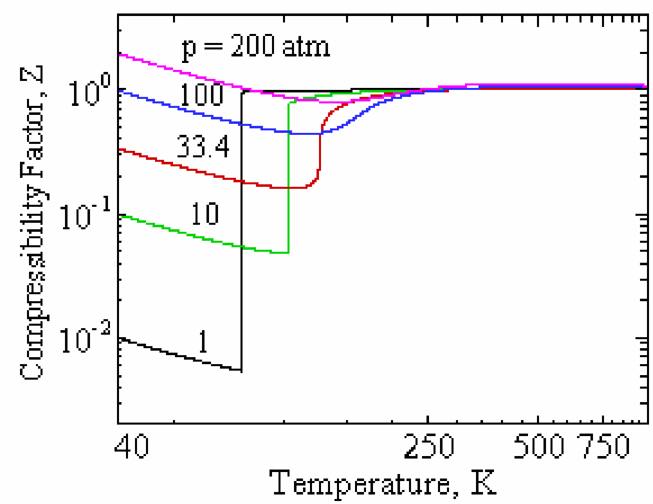

- specific heat

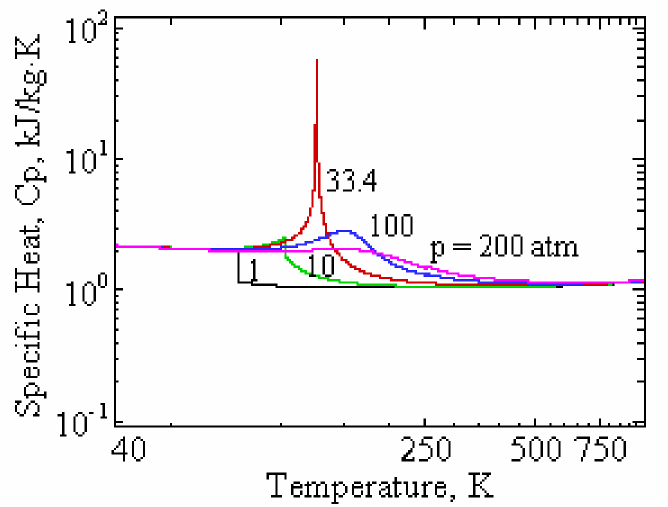

- dynamic viscosity

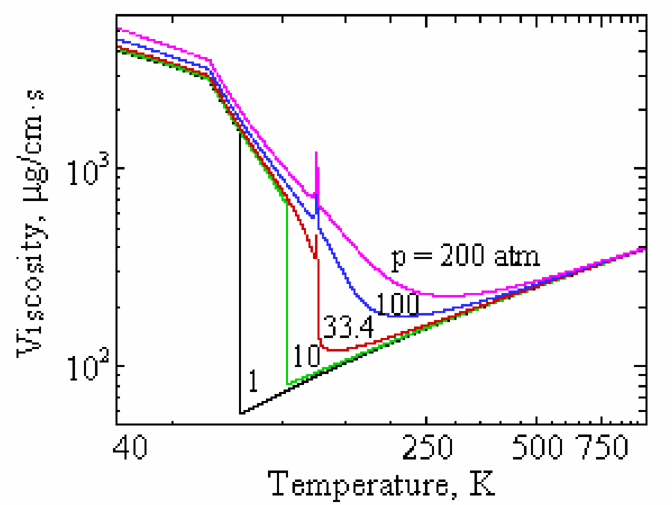

- thermal conductivity

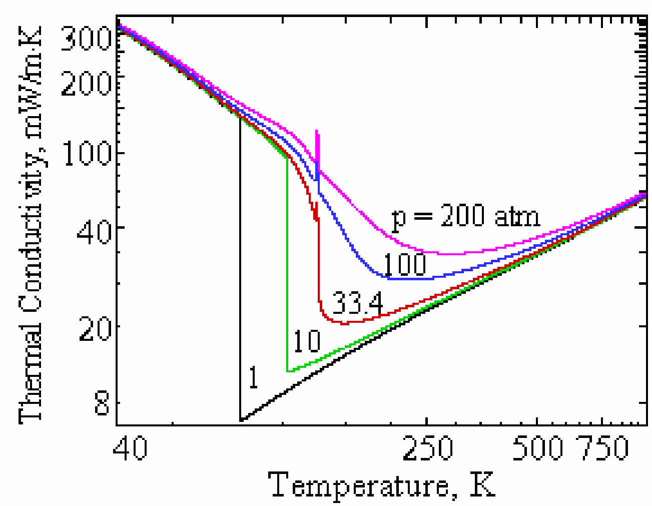

Droplet Vaporization and Combustion in Quiescent and Convective Environments

- **Liquid oxygen (LOX) droplet vaporization & combustion in hydrogen and water**

  $5 < p_\infty < 300$ atm

  $500 < T_\infty < 2500$ K

  $50 < D_0 < 300$ μm

- **Hydrocarbon droplet vaporization & combustion in air and oxygen**

  $5 < p_\infty < 200$ atm

  $300 < T_\infty < 2500$ K

  $100 < D_0 < 1000$ μm

- **Unsymmetrical dimethylhydrazine (UDMH) droplet vaporization and decomposition combustion**

  $1 < p_\infty < 180$ atm

Spherical Mode (100 atm, 0.2 m/s; t=610 μs)

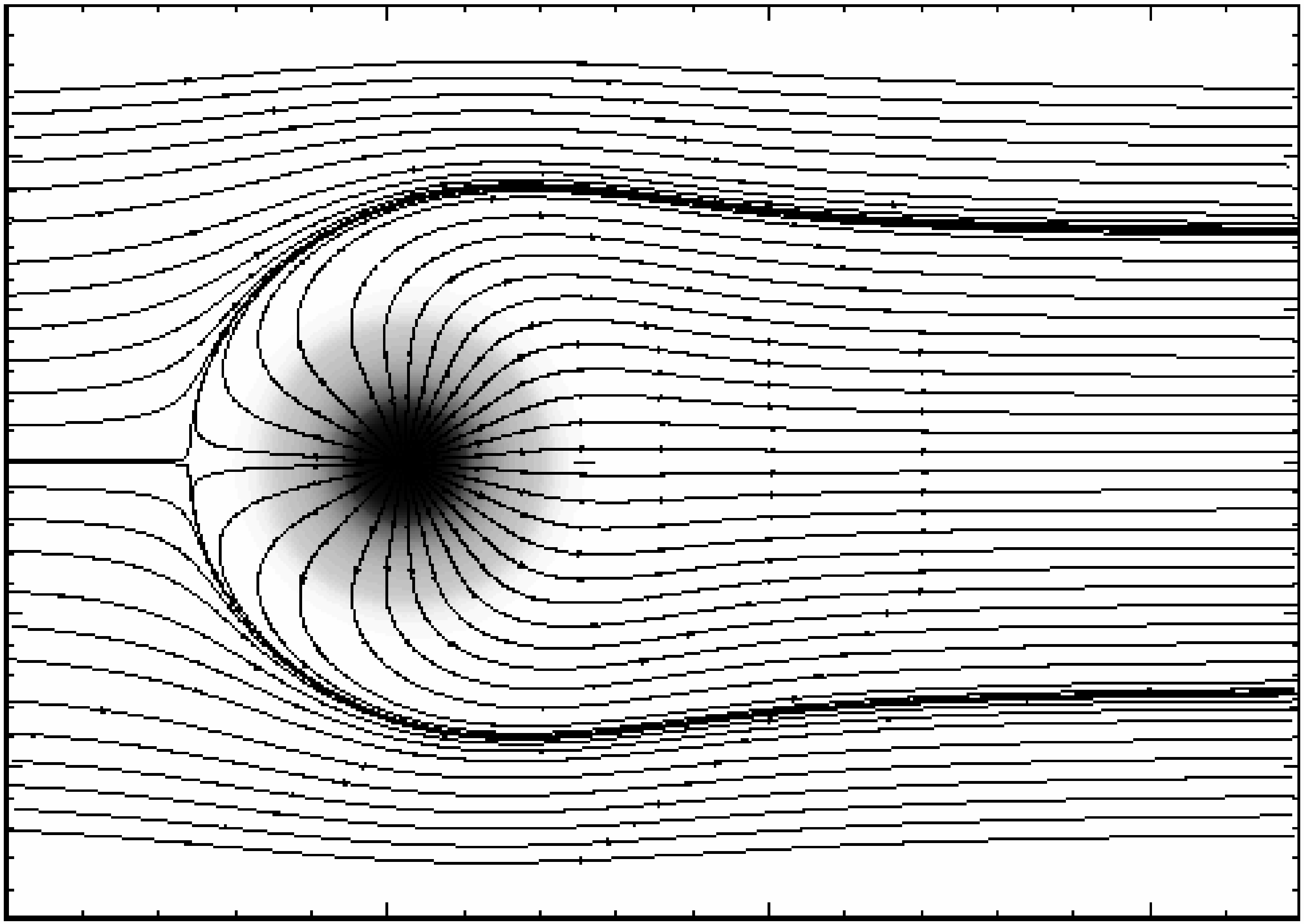

Breakup Mode (100 atm, 15 m/s; t=170 μs)

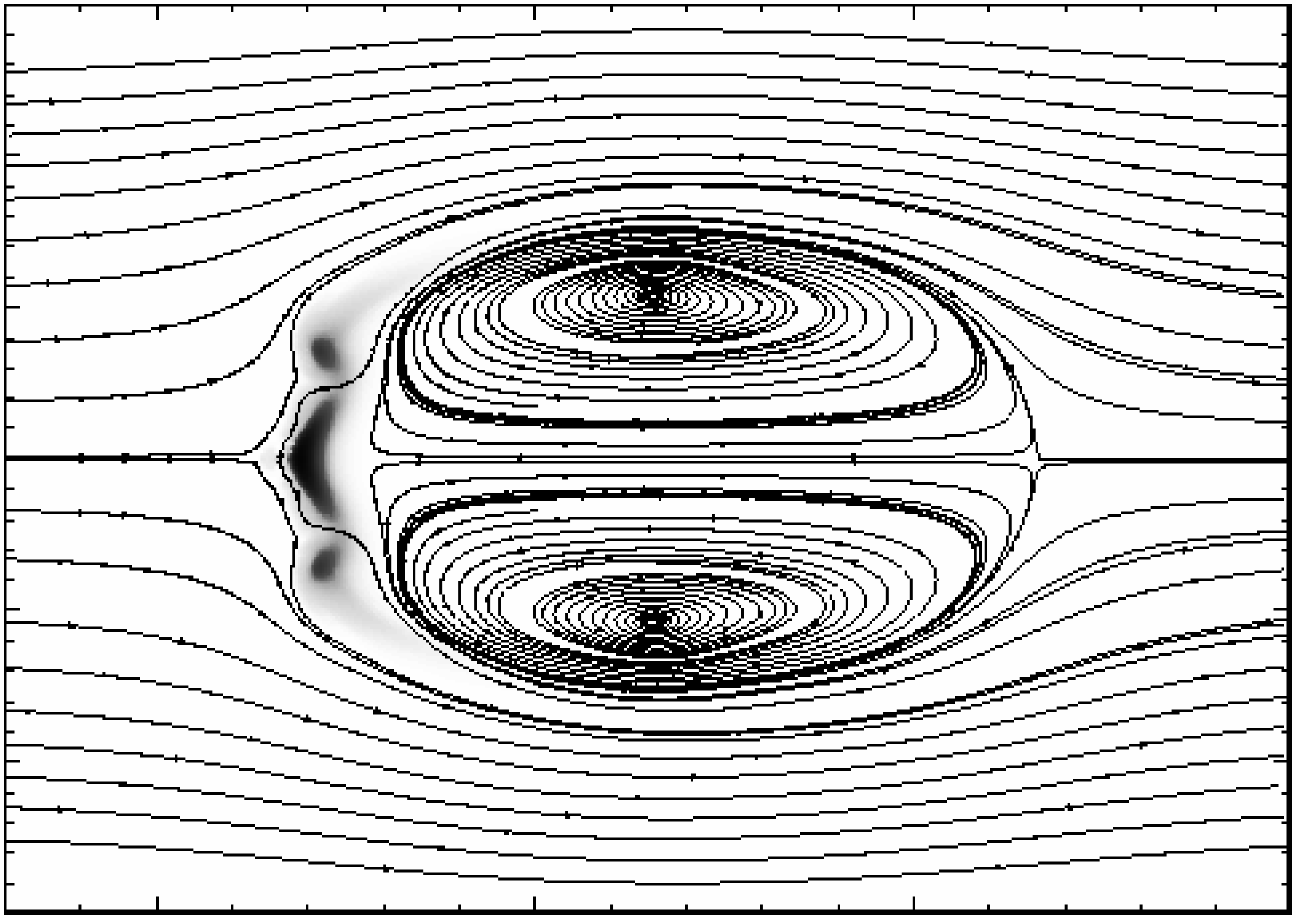

Flow and Temperature Fields

PENNSTATE 1855
Department of Mechanical & Nuclear Engineering

P_∞=100 atm, T_∞=1000 K, u_∞ =20 m/s, T_0=100 K, d_0=50 μm, H/R=8

t=8 μs

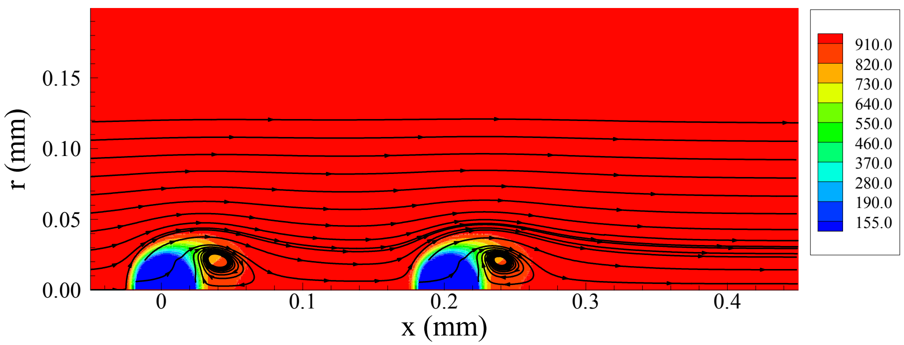

t=90 μs

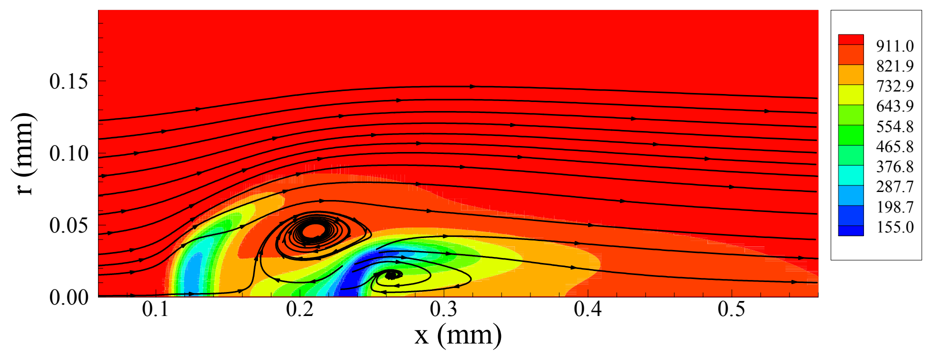

t=40 μs

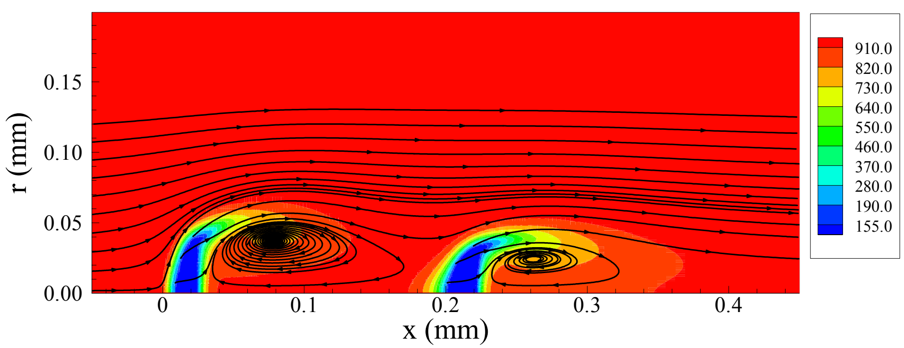

t=110 μs

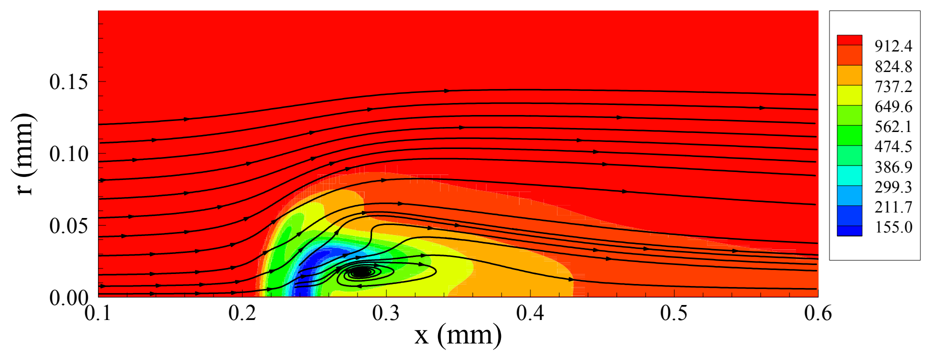

Effect of Pressure and Velocity on Droplet Lifetime

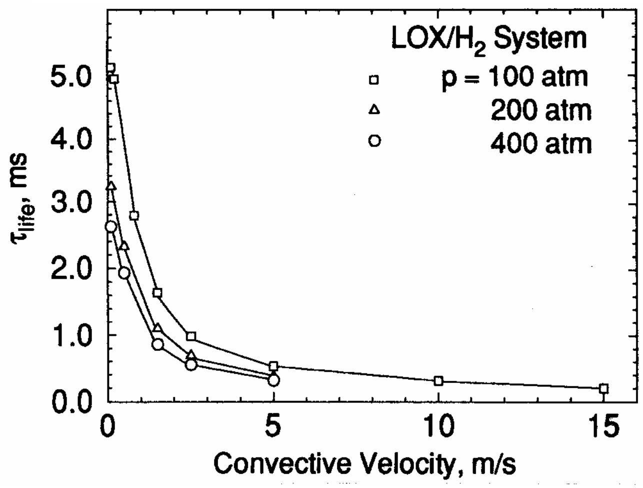

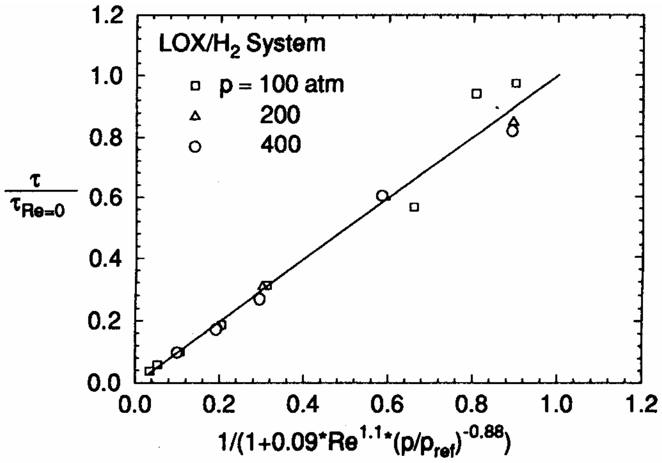

- **effect of ambient pressure on**
  - thermophysical properties
  - critical mixing state
  - convective heat transfer
- **effect of ambient velocity on**
  - convective heat transfer

- **atmospherical condition**
  - Ranz and Marshall's correlation

$$\frac{\tau_f}{\tau_{f,\mathrm{Re}=0}} \propto \frac{h_{\mathrm{Re}=0}}{h} = \frac{1}{1+0.3\,\mathrm{Re}^{1/2}\,\mathrm{Pr}^{1/3}}$$

- **supercritical condition**
  - LOX/hydrogen system

$$\frac{\tau_f}{\tau_{f,\mathrm{Re}=0}} \propto \frac{h_{\mathrm{Re}=0}}{h} = \frac{1}{1+0.15634\,\mathrm{Re}^{1.1}\,\mathrm{Pr}_{O_2}^{-0.88}}$$

Supercritical Fluid Injection

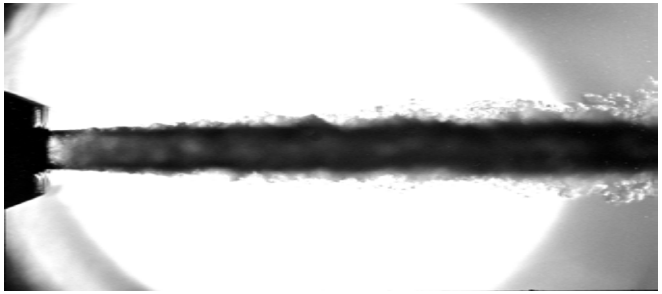

p_{ch} = 4.0 MPa
T_{LN2} = 105 K
T_{GN2} = 300 K
u_{LN2} = 10 m/s
D_{in} = 1.9 mm

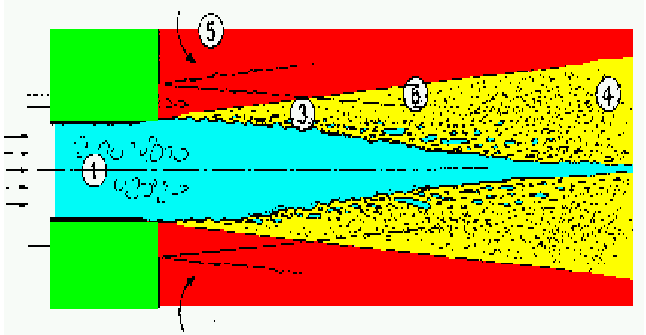

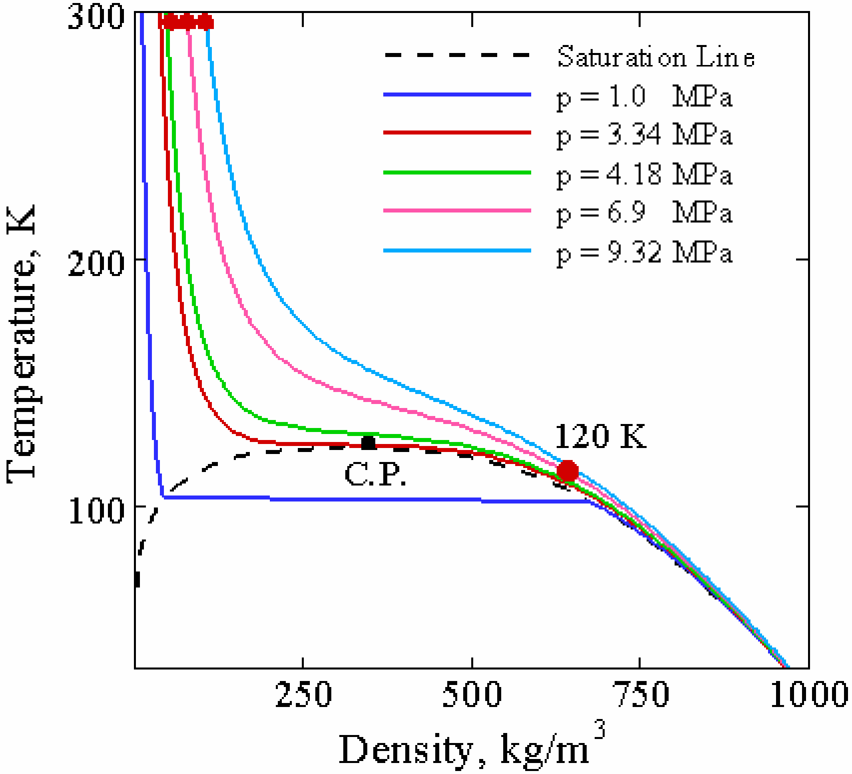

p_∞ = 3.4 - 10.0 MPa , T_∞ = 300 K,
T_{in} = 120 K , D_{in} = 0.254 mm,
u_{in} = 15 m/s, Re = 20000 – 40000

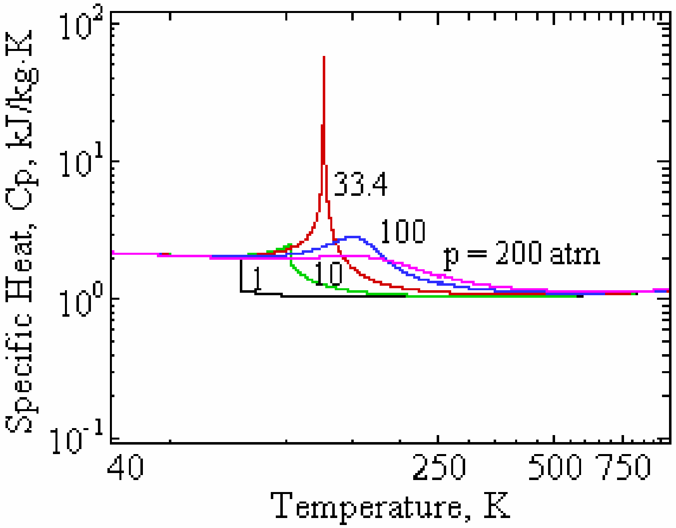

Shadowgraph Images of Cryogenic Nitrogen Injection

Mayer et al. AIAA 2001-3275

(p_∞= 6.0 MPa, T_∞= 300 K, u_{in}= 4.9 m/s, T_{in}= 132 K, D_{in}= 2.2 mm)

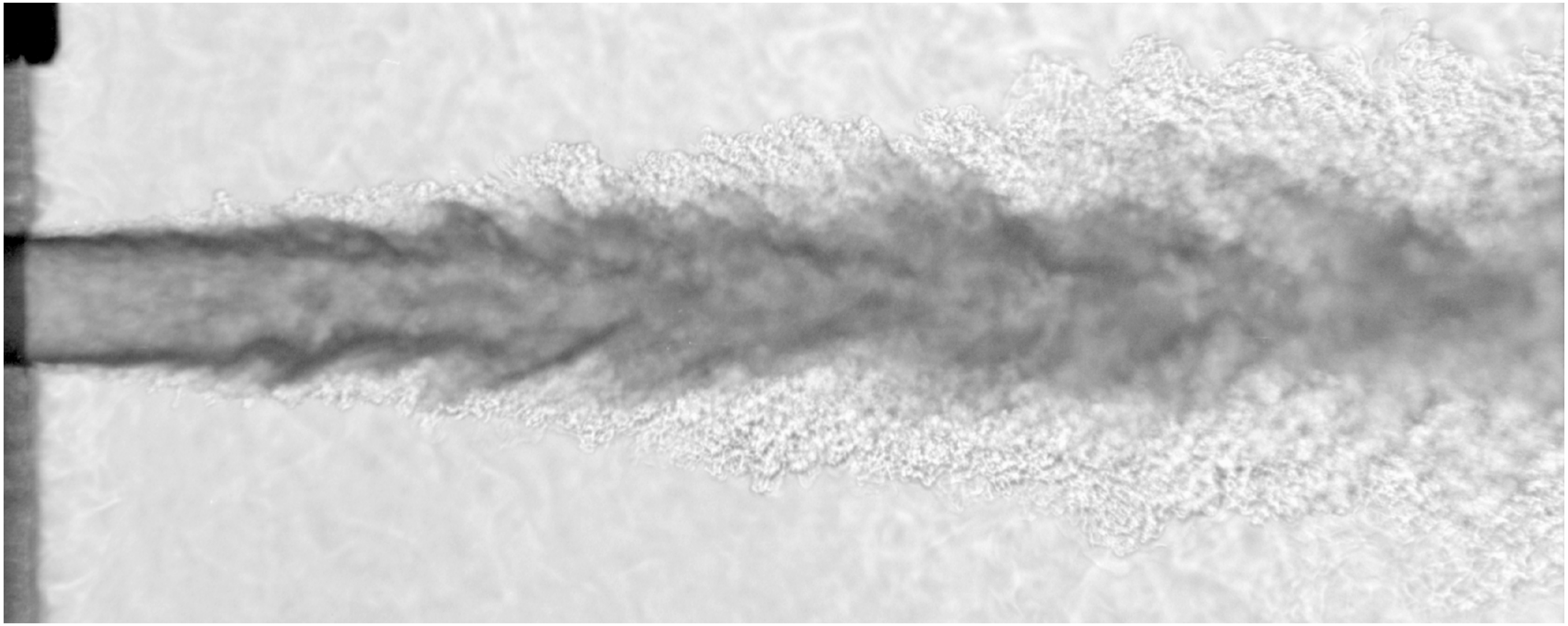

Computational Domain and Grids

PENNSTATE 1855
Department of Mechanical & Nuclear Engineering

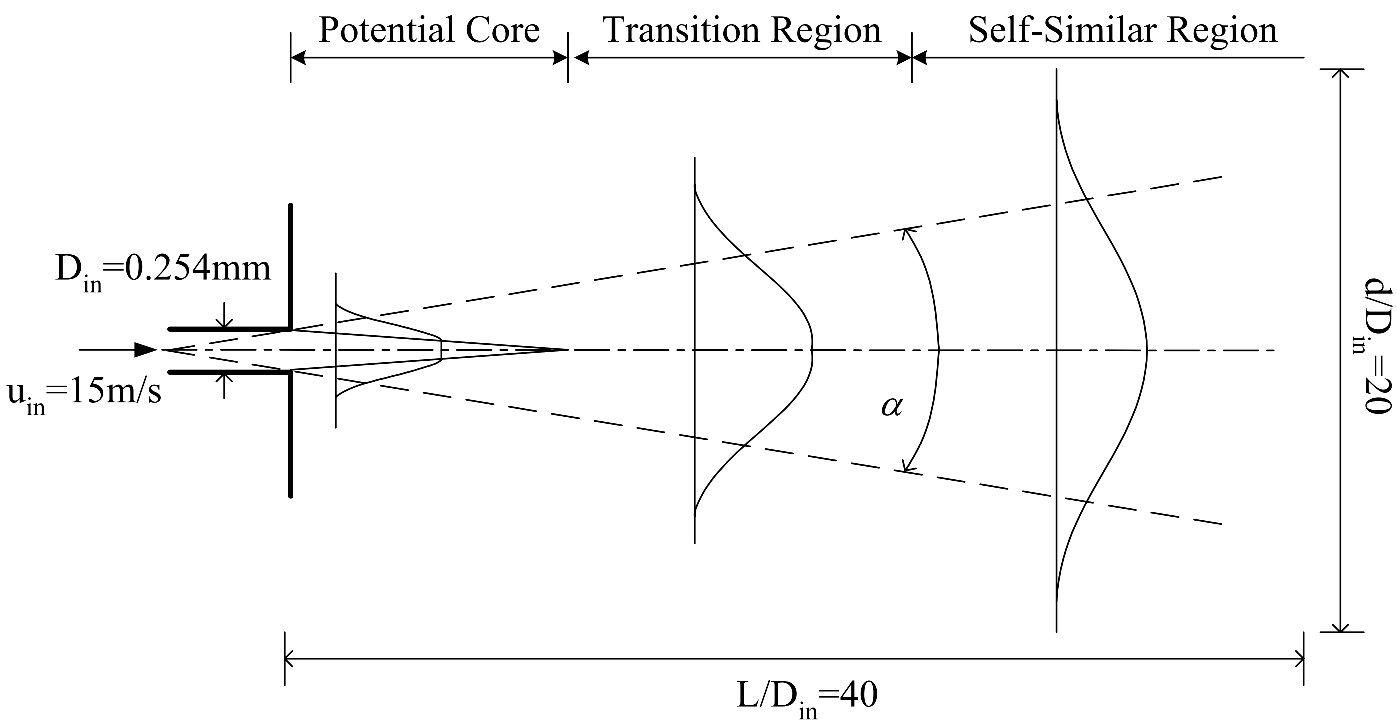

- Kolmogorov microscale $\eta_t/l_t \sim Re_t^{-3/4}$
- Taylor microscale $\lambda_t/l_t \sim Re_t^{-1/2}$
- $3.4 \le p_{ch} \le 10.0\ MPa$ and $D_{in} = 0.254\ mm$
- $3 < \lambda_t < 5\ \mu m$

total grids

$225 \times 75 \times 72 = 1{,}215{,}000$

mean grid spacing in near injector region

$\Delta = 5\ \mu m$

PENNSTATE

Density Gradient Field

Department of Mechanical & Nuclear Engineering

(p_∞= 9.3 MPa, T_∞= 300 K, u_{in}= 15 m/s, T_{in}= 120 K, D_{in}= 254 μm)

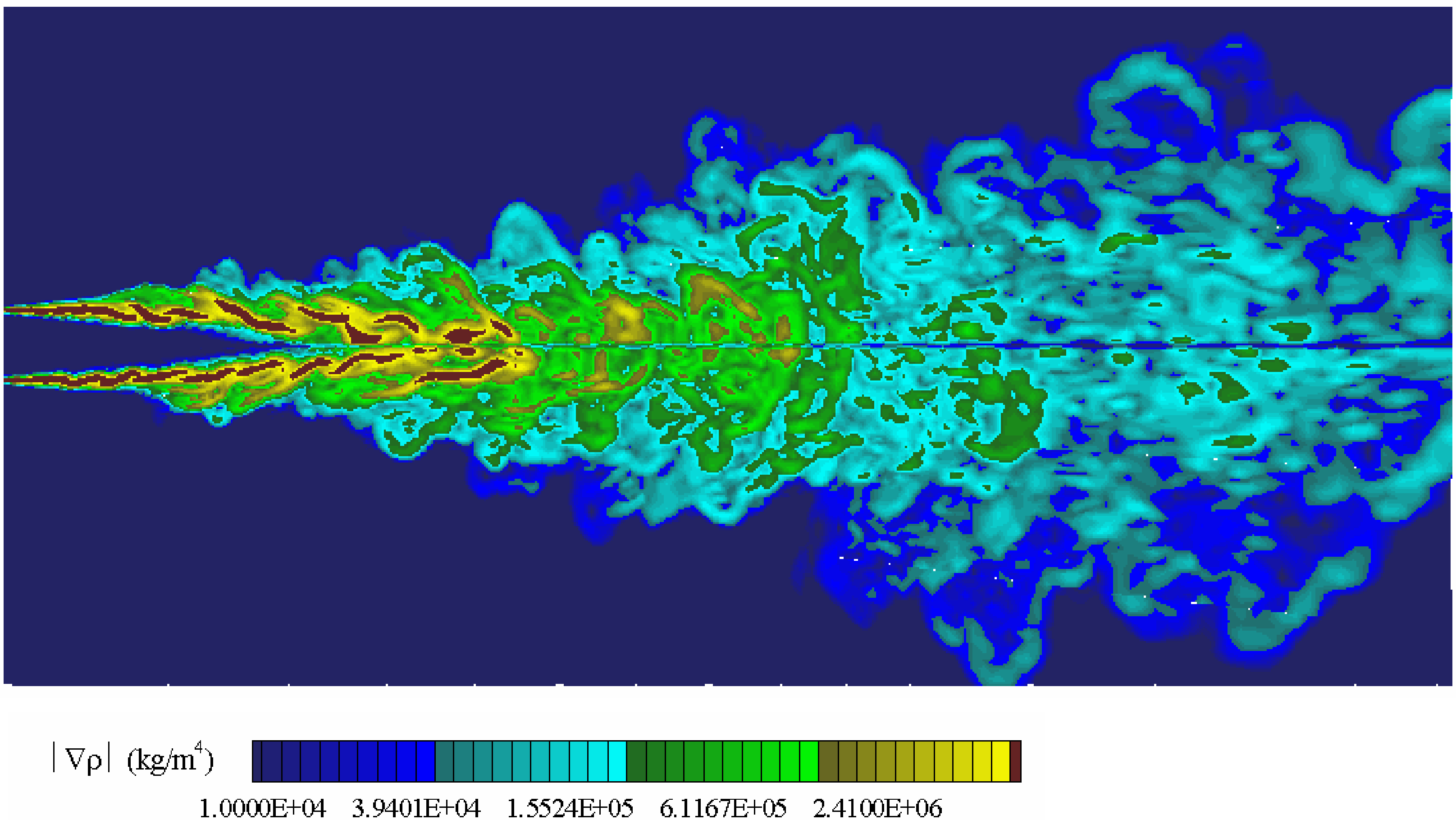

Time Evolution of Density Gradient Field

PENNSTATE
1 8 5 5
Department of Mechanical & Nuclear Engineering

(p_∞ = 6.9 MPa, T_∞ = 300 K, u_{in} = 15 m/s, T_{in} = 120 K, D_{in} = 254 μm)

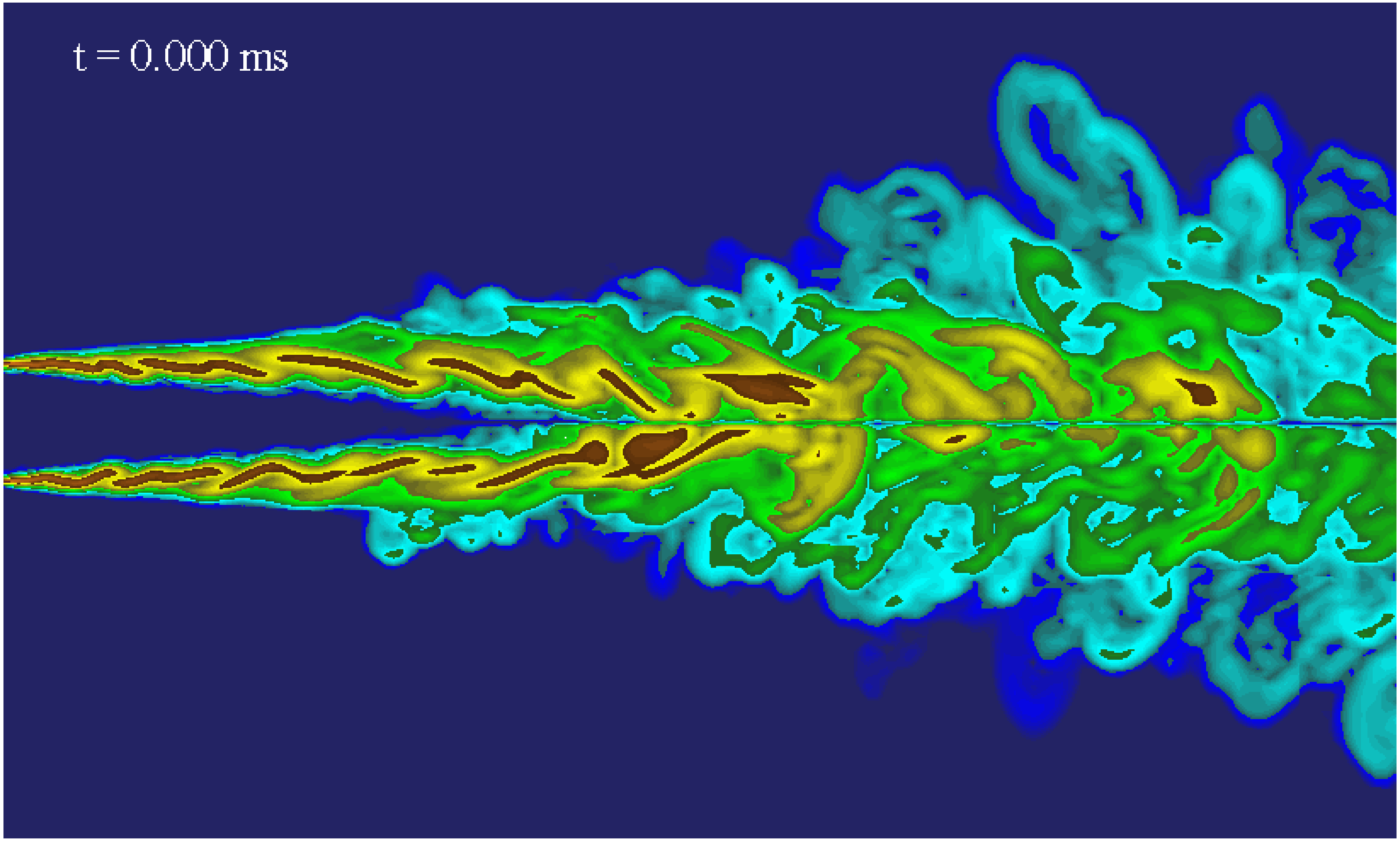

Snapshots of Density and Temperature Gradient Fields

PENNSTATE 1855
Department of Mechanical & Nuclear Engineering

(p_∞= 9.3MPa, T_∞= 300K, u_{in}= 15m/s, T_{in}= 120K, t= 1.550ms, D_{in}= 254μm)

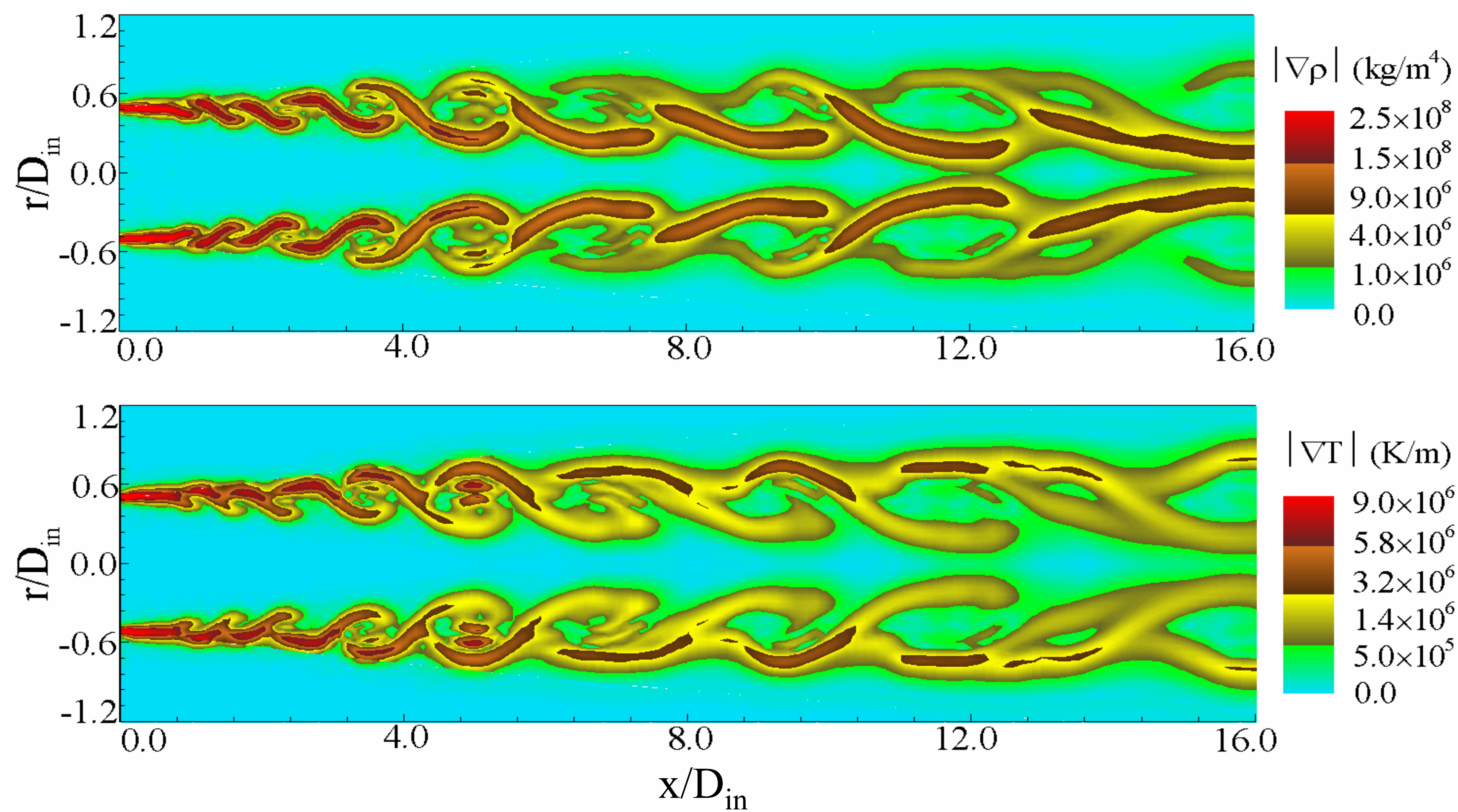

Most Energy Containing POD Modes of Axial Velocity

(p_∞= 9.3 MPa, T_∞= 300 K, u_{in}= 15 m/s, T_{in}= 120 K, D_{in}= 254 μm)

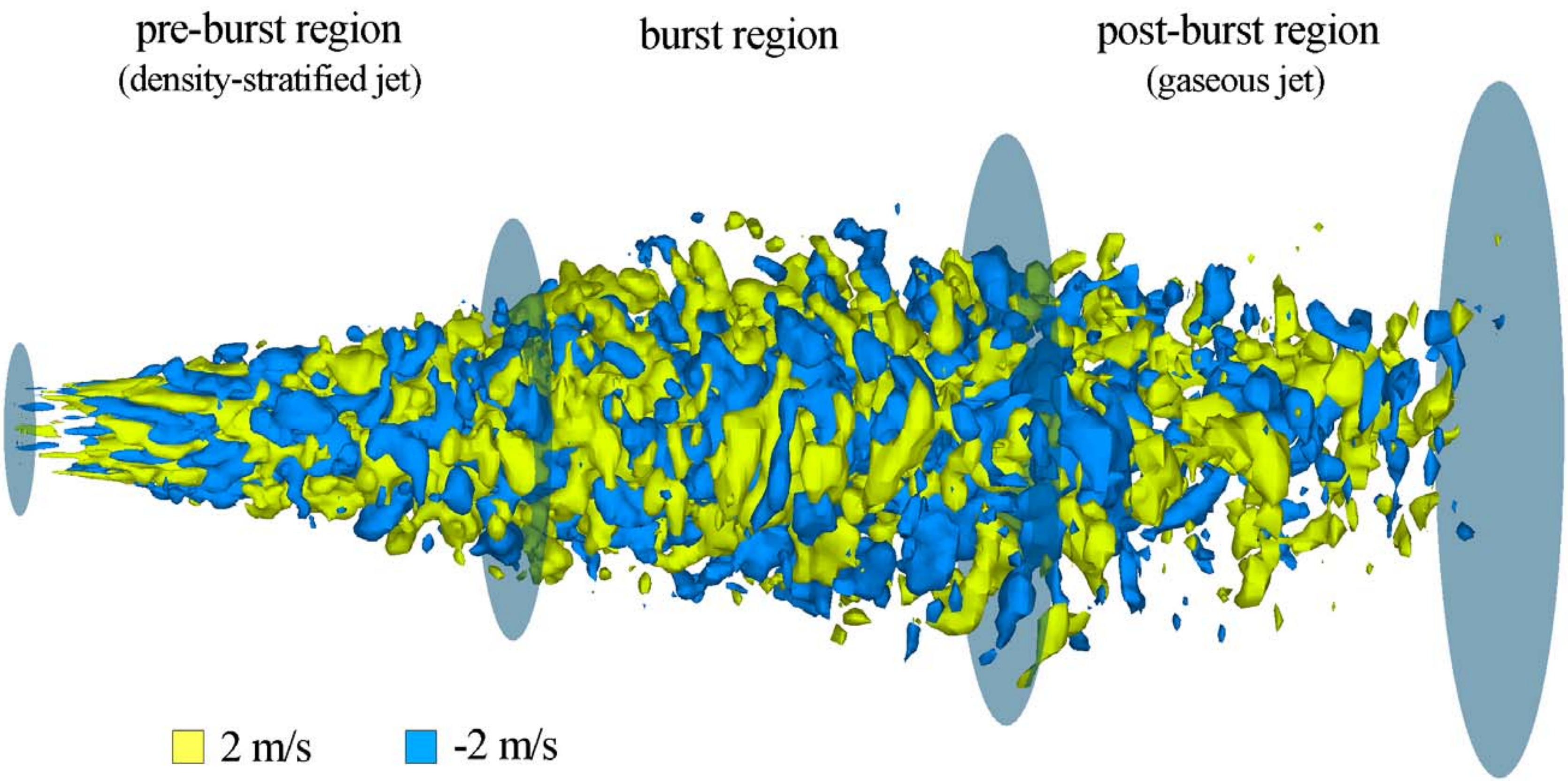

Iso-Surfaces of Pressure and Density Gradients

PENNSTATE 1855
Department of Mechanical & Nuclear Engineering

(p_∞ = 9.3 MPa, T_∞ = 300 K, u_{in} = 15 m/s, T_{in} = 120 K, D_{in} = 254 μm)

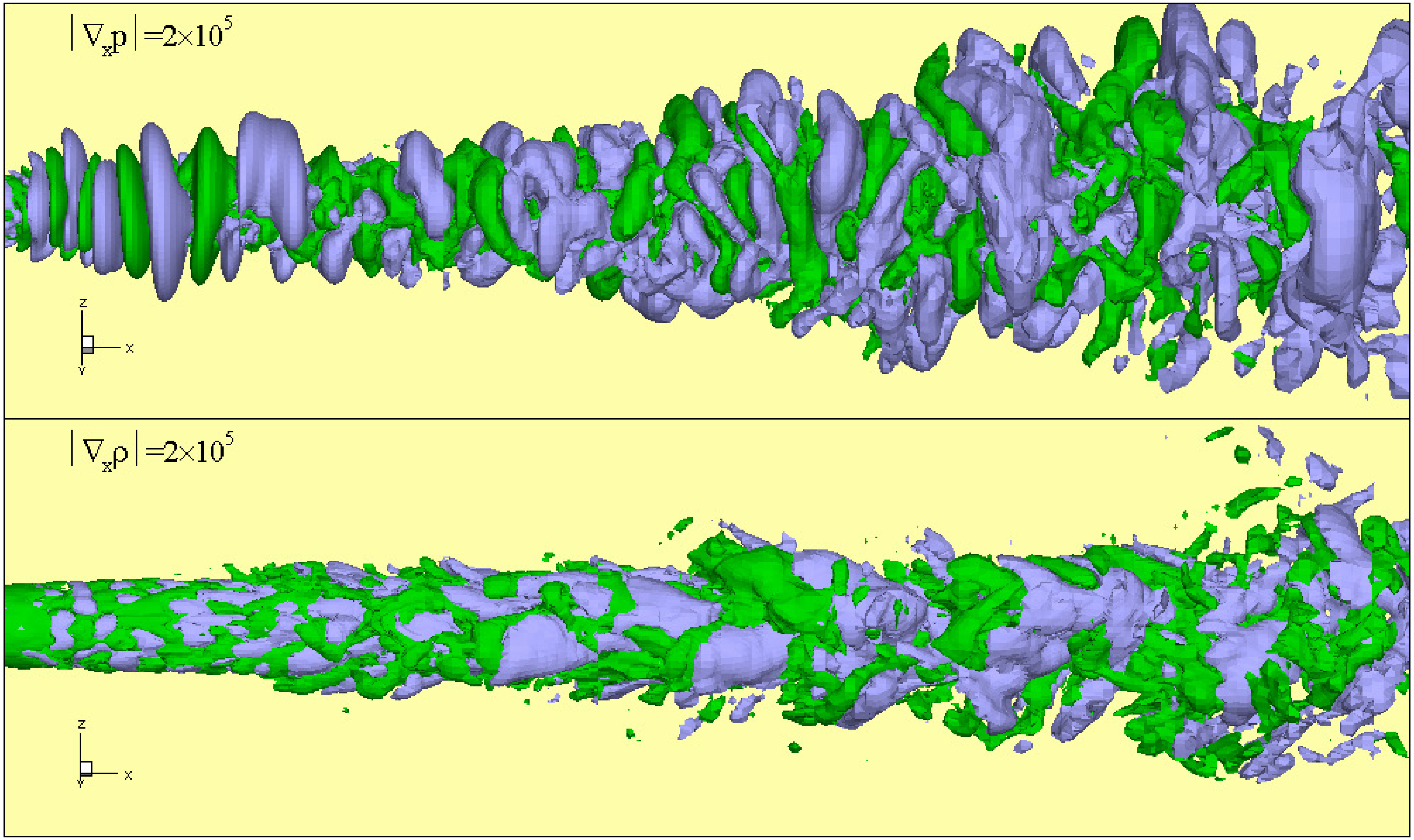

PENNSTATE

1 8 5 5

Effect of Pressure on Density and Temperature Fields

Department of Mechanical & Nuclear Engineering

$T_\infty = 300K$, $u_{in} = 15m/s$, $T_{in} = 120K$, $D_{in} = 254\mu m$)

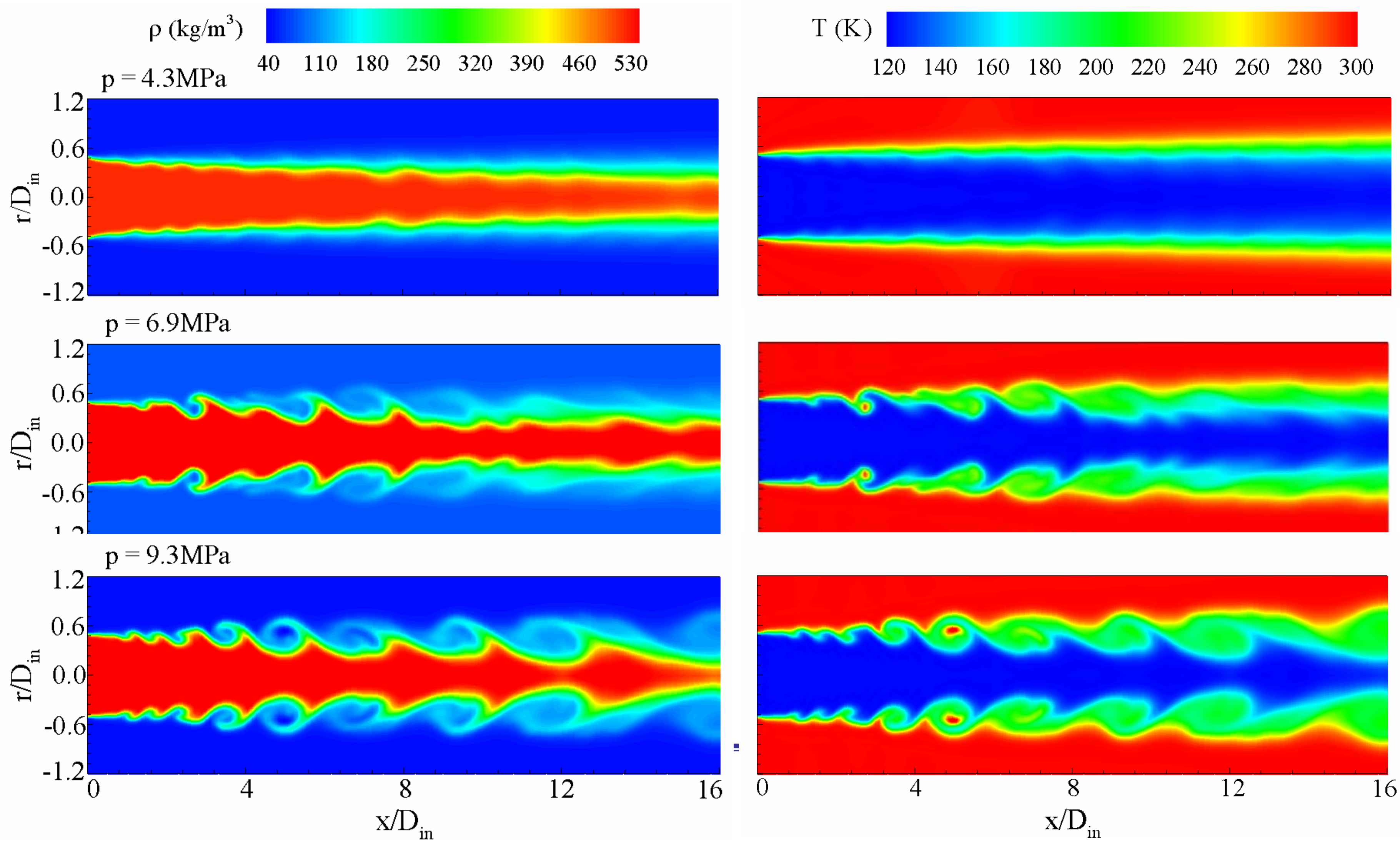

Power Spectral Densities of Velocity Fluctuations

(p_∞= 9.3MPa, T_∞= 300K, u_{in}= 15m/s, T_{in}= 120K, D_{in}= 254μm)

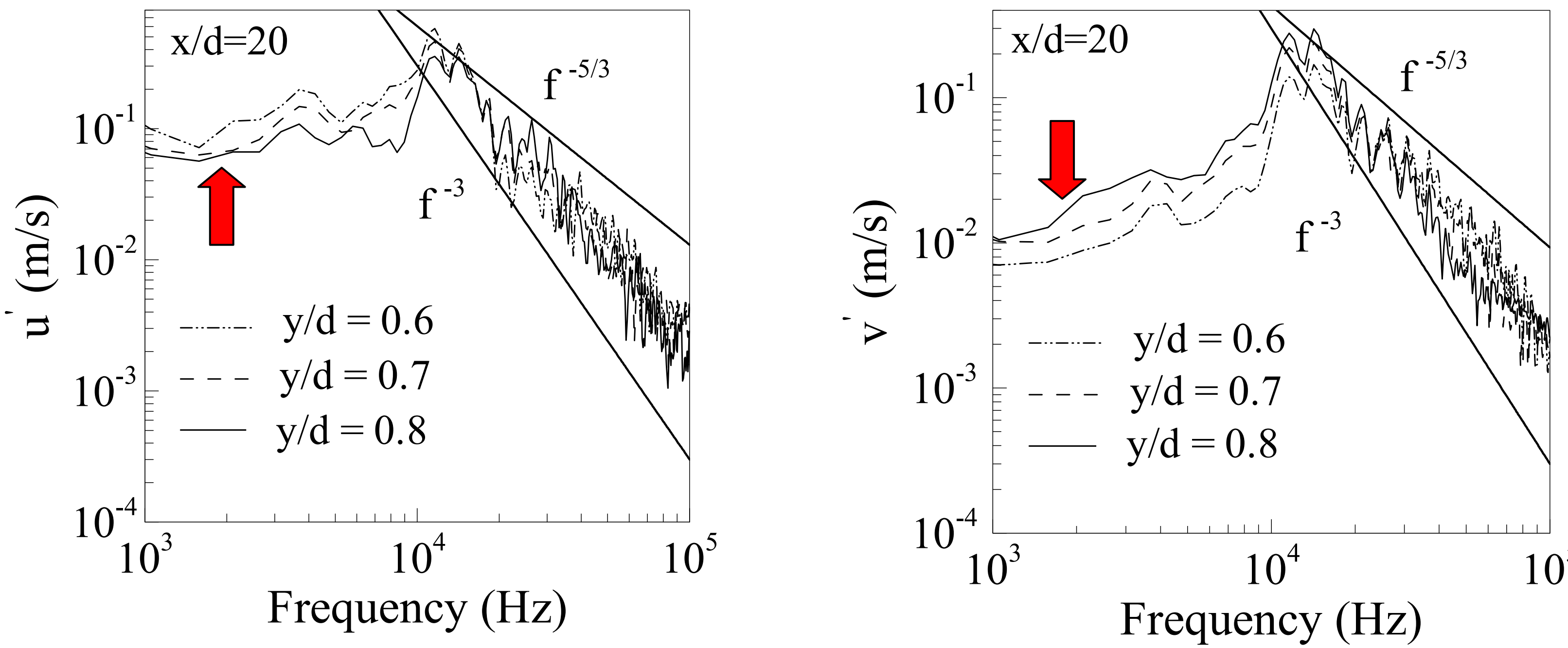

Large density-gradient regions act like a solid wall that amplifies the axial turbulent fluctuation but damps the radial one.

Vortex Shedding Frequency

(p_∞= 9.3MPa, T_∞= 300K, u_{in}= 15m/s, T_{in}= 120K, D_{in}= 254μm)

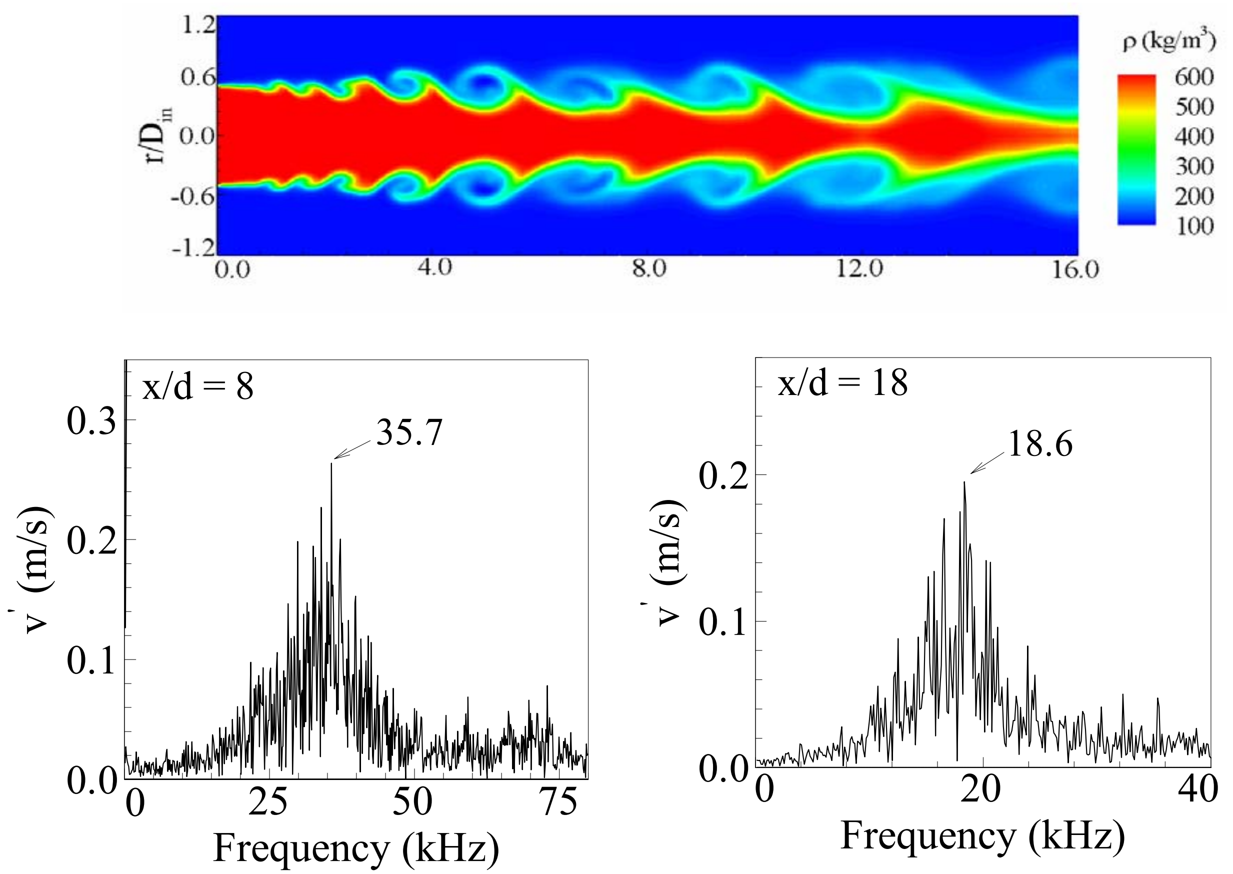

Jet flow instability analysis

$$St_j = f_j \theta_0 / \bar{U}$$

where $0.044 \le St_j \le 0.048$

$$\bar{U} = 15 \quad m/s$$

Momentum thickness

$$\theta_0 = 0.02 \quad mm$$

$$\theta_0 = \int_0^\infty \frac{u}{U_{max}}\left(1 - \frac{u}{U_{max}}\right)dy$$

choose

$$St_j = 0.046$$

then

$$f_1 = 34500$$

$$f_2 = 17250$$

Linear Stability Analysis of Real Fluid Jet

PENNSTATE 1855
Department of Mechanical & Nuclear Engineering

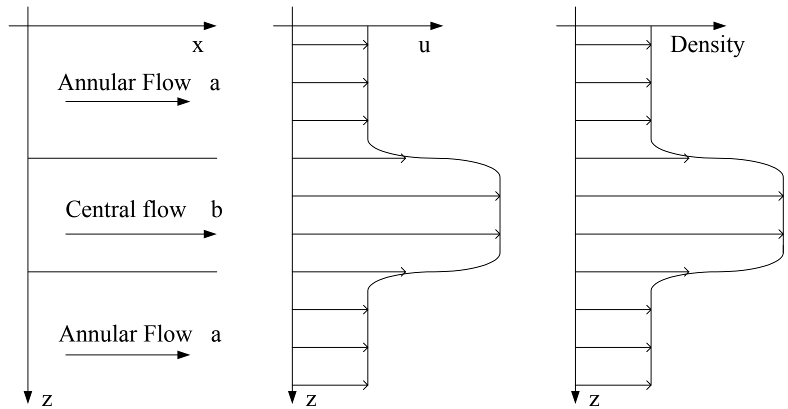

Approach

- Two-dimensional fluid jet instability at supercritical conditions.
- Unified treatment of real-fluid thermodynamics and transport phenomena.
- Disperse equation solved by Newton-Ralpson method.

Conclusions

- As the density ratio increases, the spatial growth rate of the interfacial instability wave decreases. ➡ Density stratification tends to stabilize the mixing layer.
- Density stratification has little effect on the frequency of the most unstable mode.

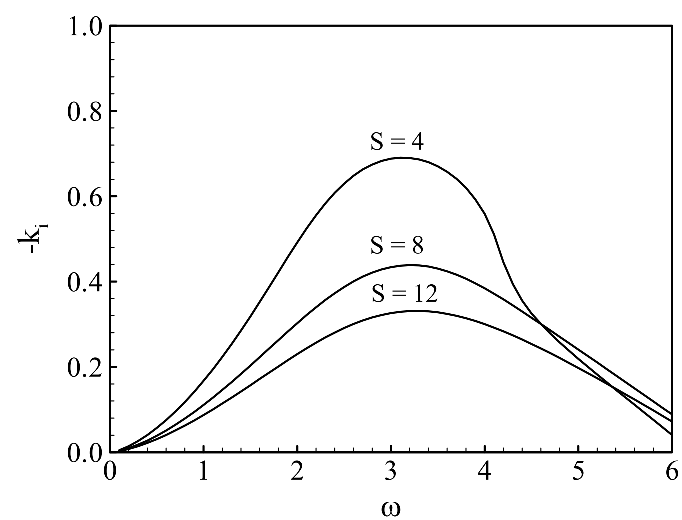

PENNSTATE
1 8 5 5
Department of Mechanical & Nuclear Engineering

Bi-Propellant Swirl Co-Axial Injector

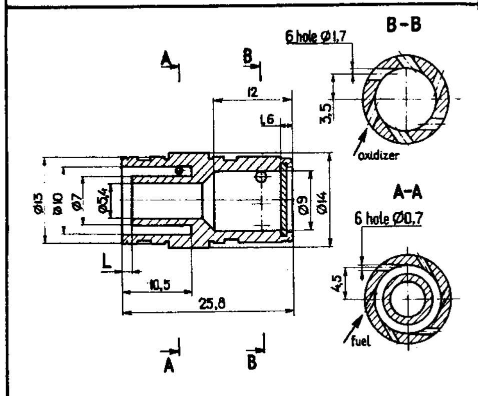

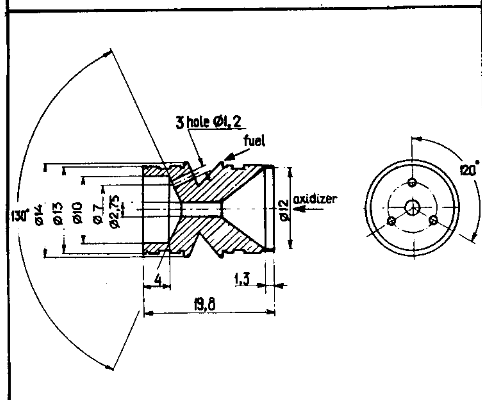

Component	Geometrical characteristic	Spray-cone angle	Pressure drop	flow rate
	–	angle degrees	MPa	g/sec.
oxidizer	2	80	0,426	172,9
fuel	24,5	135	0,696	64,8
oxidizer	–	–	0,426	172,3
fuel	–	–	0,696	64, 8

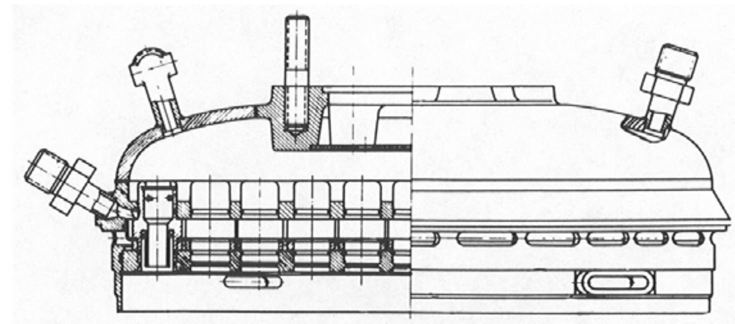

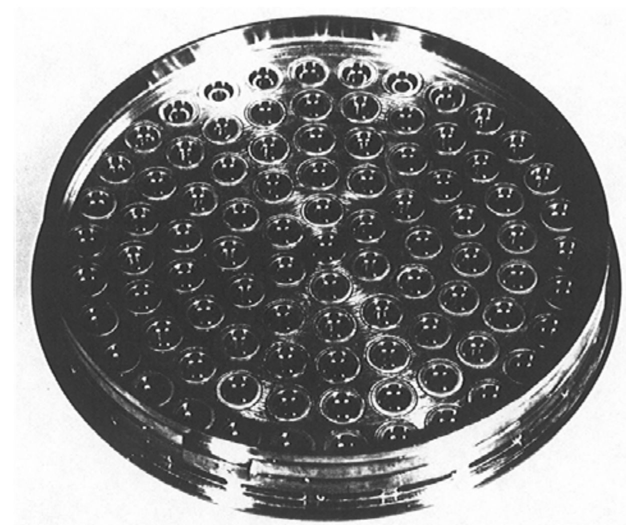

Large Eddy Simulation of Swirling Oxygen Jet

PENNSTATE 1855
Department of Mechanical & Nuclear Engineering

Issues

- Swirling jet dynamics at supercritical conditions.
- Flame stabilization mechanisms of swirl co-axial injector.
- Liquid rocket thrust chamber dynamics.

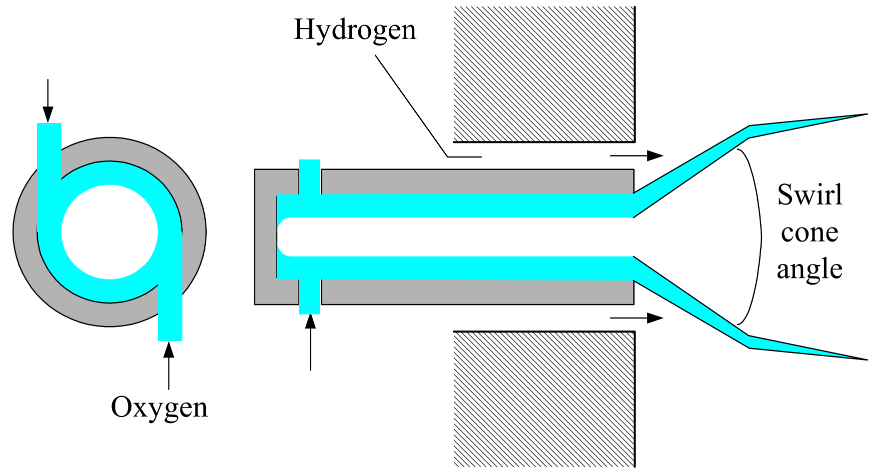

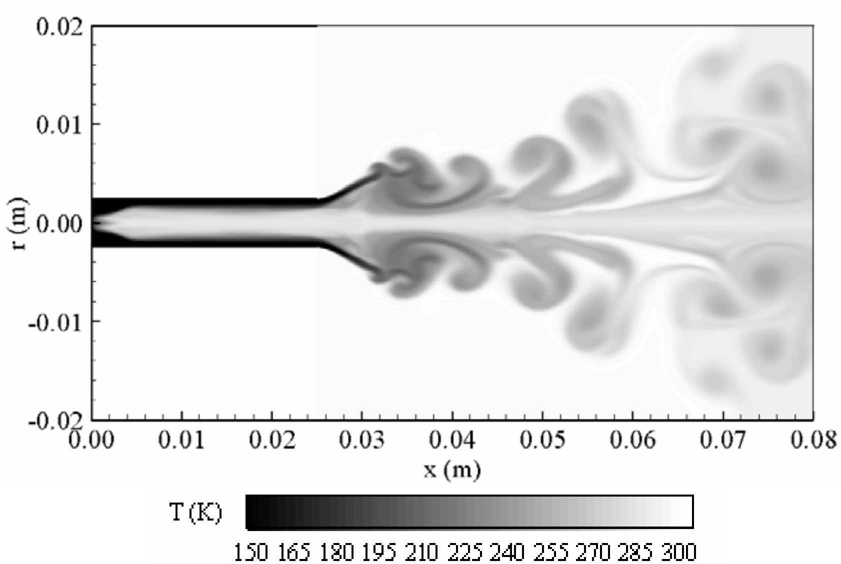

Major Results

- Liquid film thickness and swirl cone angle.
- Detailed flow structures, including central recirculation zone, surface instability, etc.
- Response of injector dynamics to external forcing.

LOX/Kerosene Preburner Swirl Injector

(Wu, et al., unpublished data, 2003)

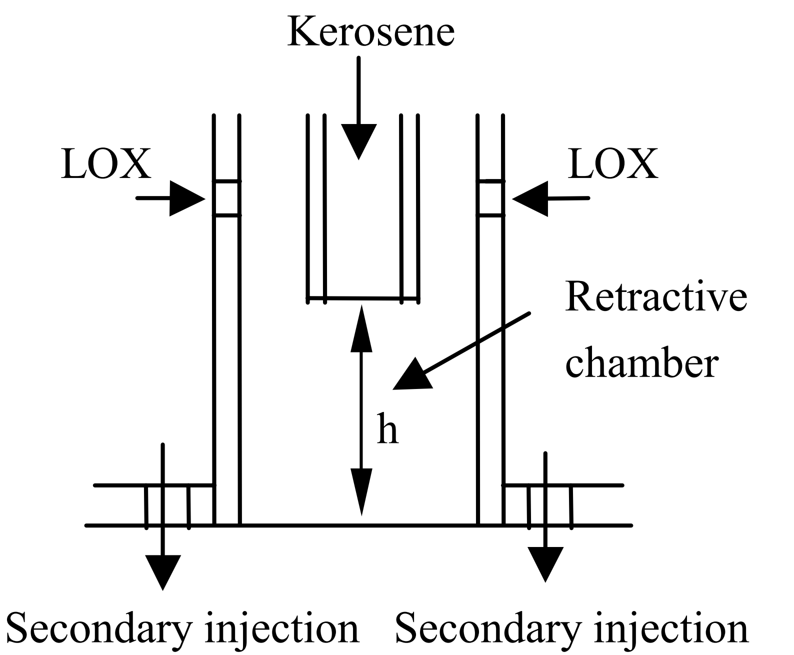

oxidizer-rich preburner injector

damaged inner centrifugal injector

Time Evolution of Swirling Jet

PENNSTATE
1 8 5 5
Department of Mechanical & Nuclear Engineering

(p_∞=10.0 MPa, T_∞=300 K, u_{inj}= 30 m/s, T_{inj}= 120 K, θ=30°, nitrogen)

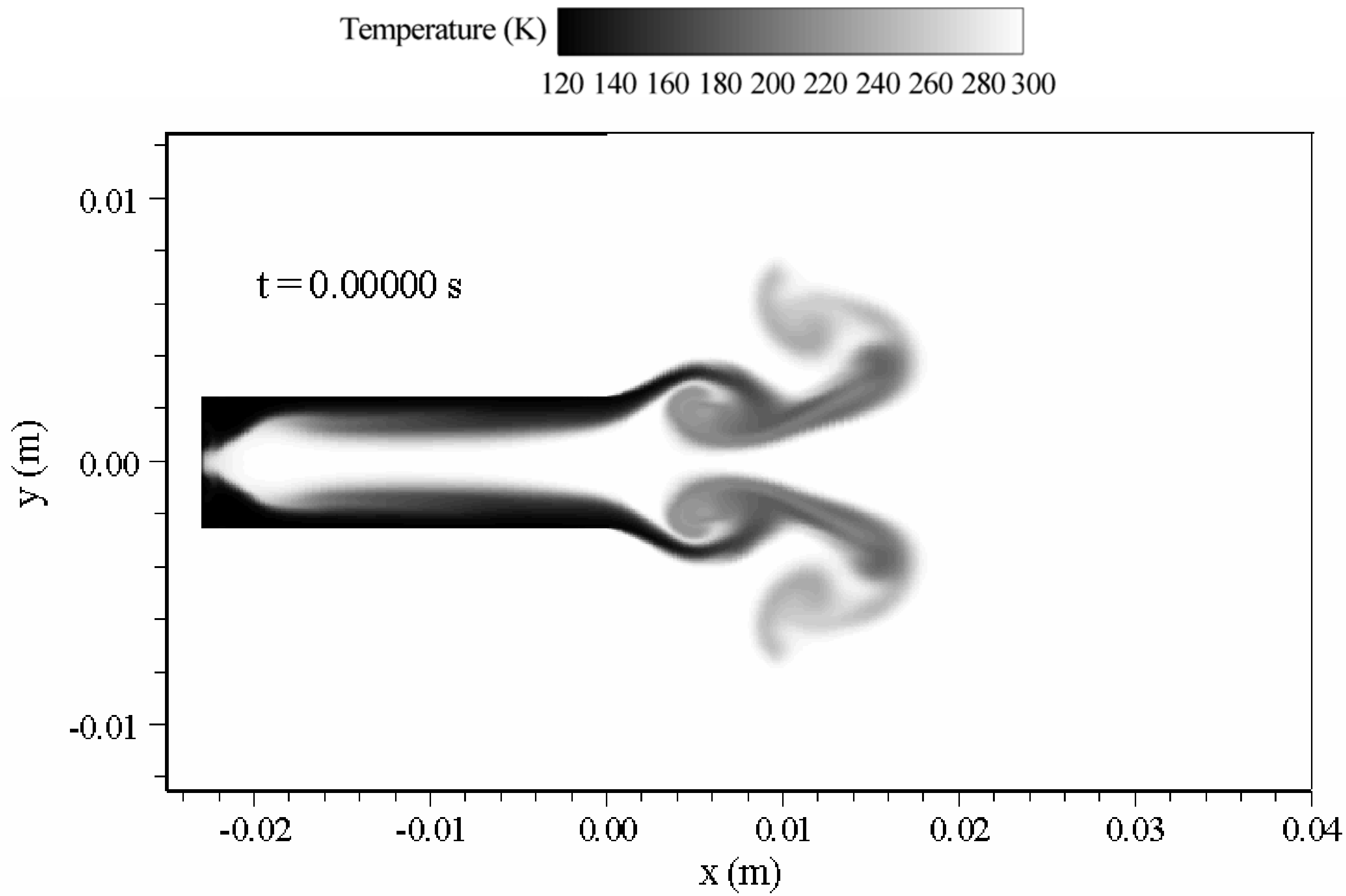

Time Evolution of Swirling Jet

Department of Mechanical & Nuclear Engineering

(p_∞=10.0 MPa, T_∞=300 K, u_{inj}= 30 m/s, T_{inj}= 120 K, θ=30°, nitrogen)

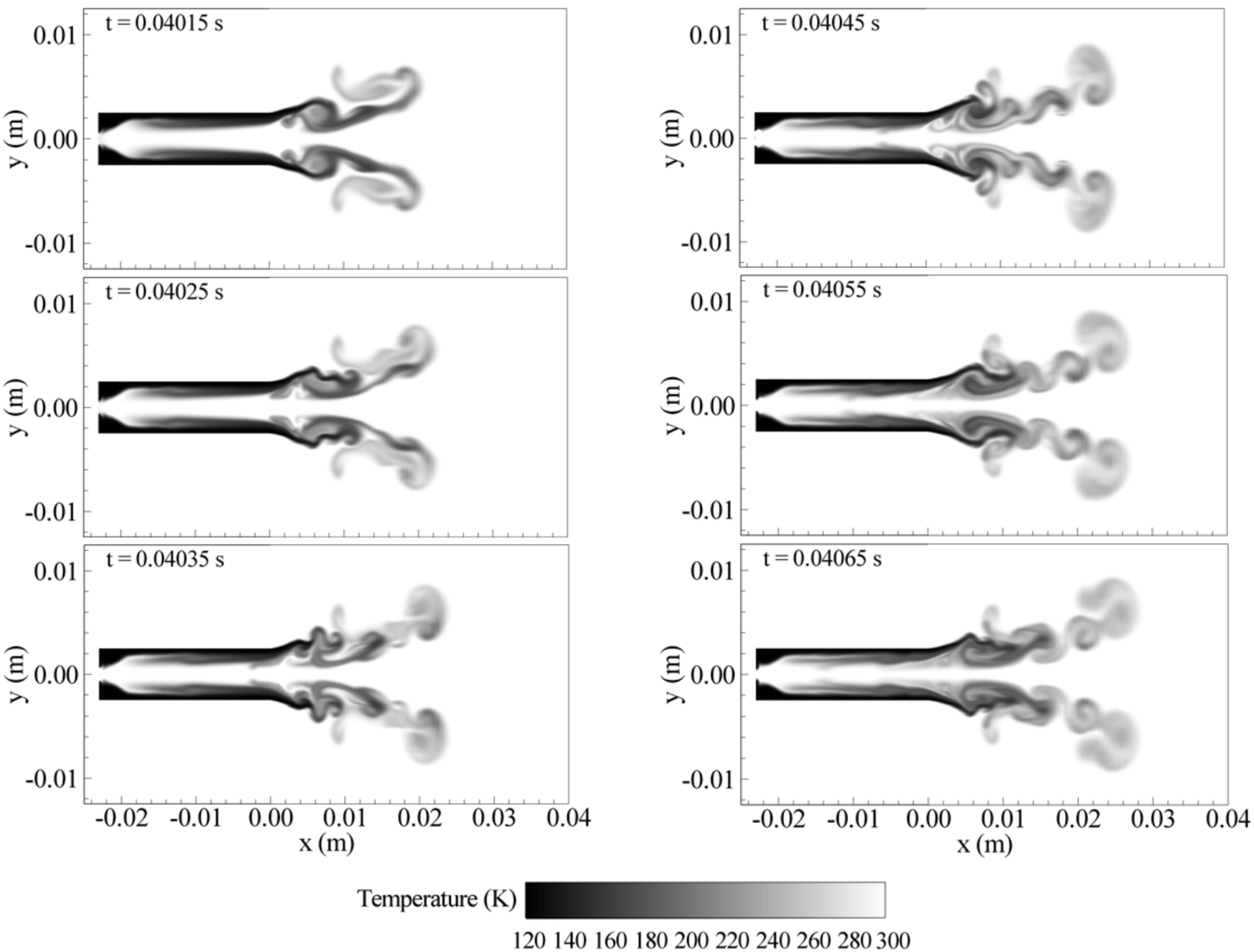

Disintegration of Swirling Water Jet
(Inamura, Tamura and Sakamoto, JPP, 2003)

Water Injection, L/D=11.67, K=1.0

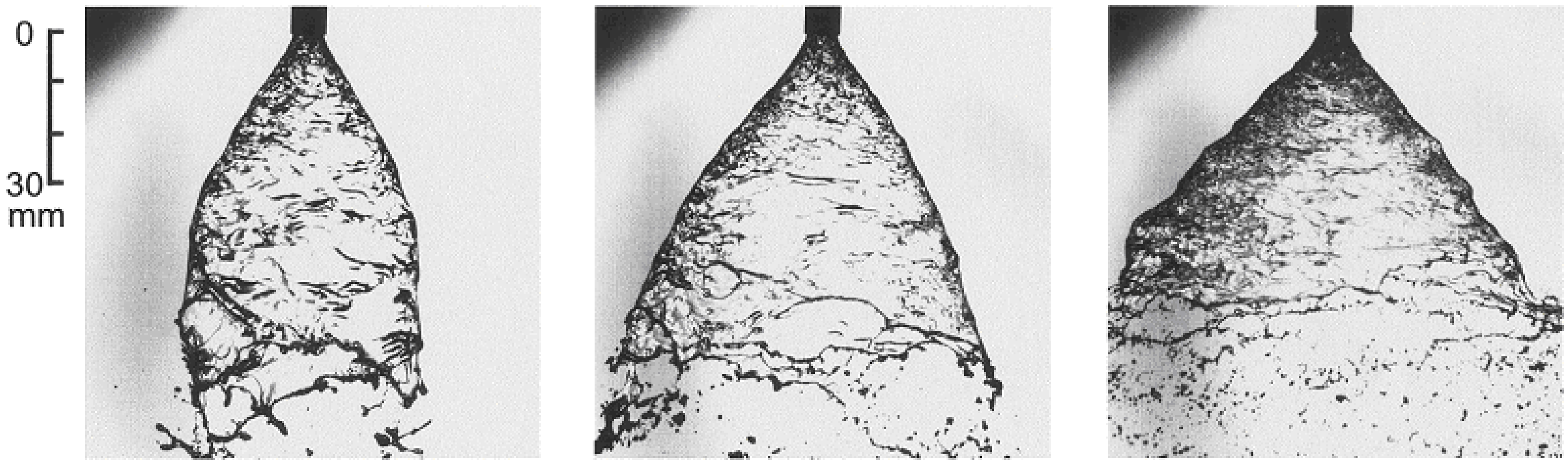

(1) M_l =26.1 g/s (2) M_l =32.5 g/s (3) M_l =48.6 g/s

- A hollow cone sheet forms around the injector exit.
- The conical sheet fluctuates vigorously and disintegrates into ligaments and droplets at the sheet tip.
- The sheet breakup point approaches the injector as the liquid flow rate increases.

PENNSTATE

1 8 5 5

Theoretical Analysis of Swirl Injector (1/2)

Department of Mechanical & Nuclear Engineering

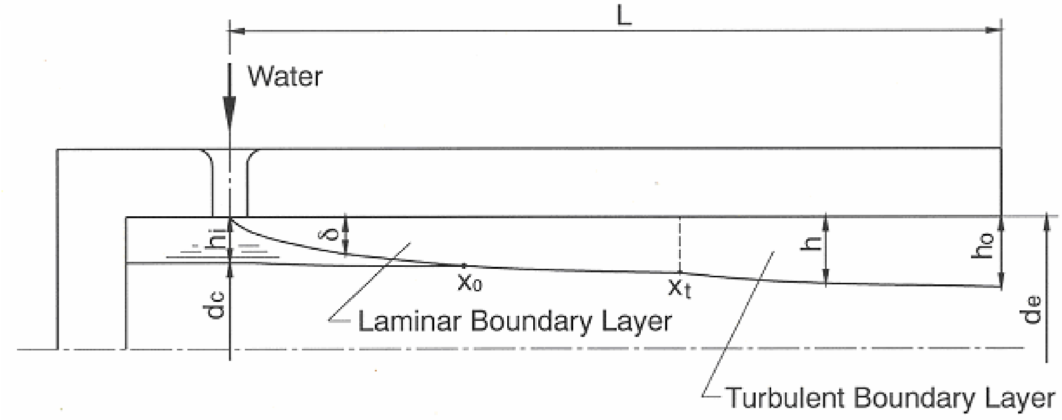

(Inamura et al. *JPP*, 2003)

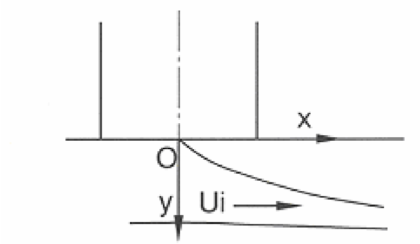

Coordinate System

$x < x_0$

$$\frac{d}{dx}\int_0^{\delta}(U_i u - u^2)dy = \frac{\tau_w}{\rho_l}$$ where $$\tau_w = \rho_l v_l (\frac{\partial u}{\partial y})_{y=0}$$ and $$\delta^* = 5.84\sqrt{x^* / \mathrm{Re}}$$

$$Q = U_i h_i = \int_0^{\delta} u dy + U_i(h-\delta)$$ $\Rightarrow$ $$h^* = 1 + (3/10)\delta^*$$

Theoretical Analysis of Swirl Injector (2/2)

$x_0 < x < x_t$

$$h^* = 1.429/\{1 + A(x^* - x_0^*)\} \qquad A = 1.682(\nu_l / Q)$$

$x_t < x$

$$h^* = 0.02798(x^*/\mathrm{Re}^{1/4}) + C_1 \qquad x_0^* = 0.0598\,\mathrm{Re}$$

$$C_1 = 1.429\{1 + A(x_t^* - x_0^*)\} - 0.0279(x_t^*/\mathrm{Re}^{1/4})$$

$x_t < x < x_0$

$$h^* = 0.02798(x^*/\mathrm{Re}^{1/4}) + C_3$$

$$C_3 = 1.143 - 0.02798(x_0^*/\mathrm{Re}^{1/4})$$

$$x_0^* = \{(1.182 - C_2)/0.2893\}\,\mathrm{Re}^{1/4}$$

Film Thickness at Post Exit

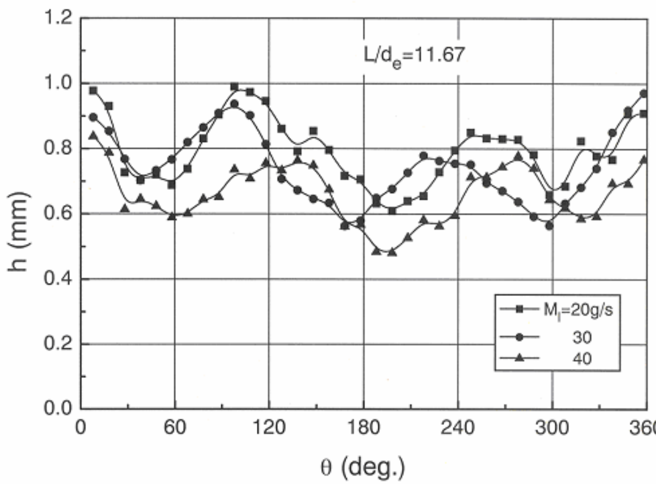

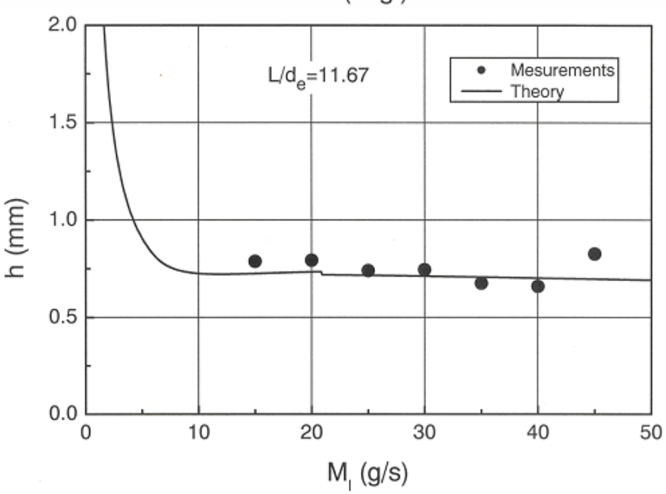

Limiting Extremes: 2) Diffusion Processes Dominate

- "High" Heating Rates
  - diminished intermolecular forces promote diffusion processes prior to atomization
  - injected jet vaporizes forming continous fluid in presence of exceedingly large interfacial gradients
  - diffusion flame resides within annular post wake separating oxygen jet from outer hydrogen flow

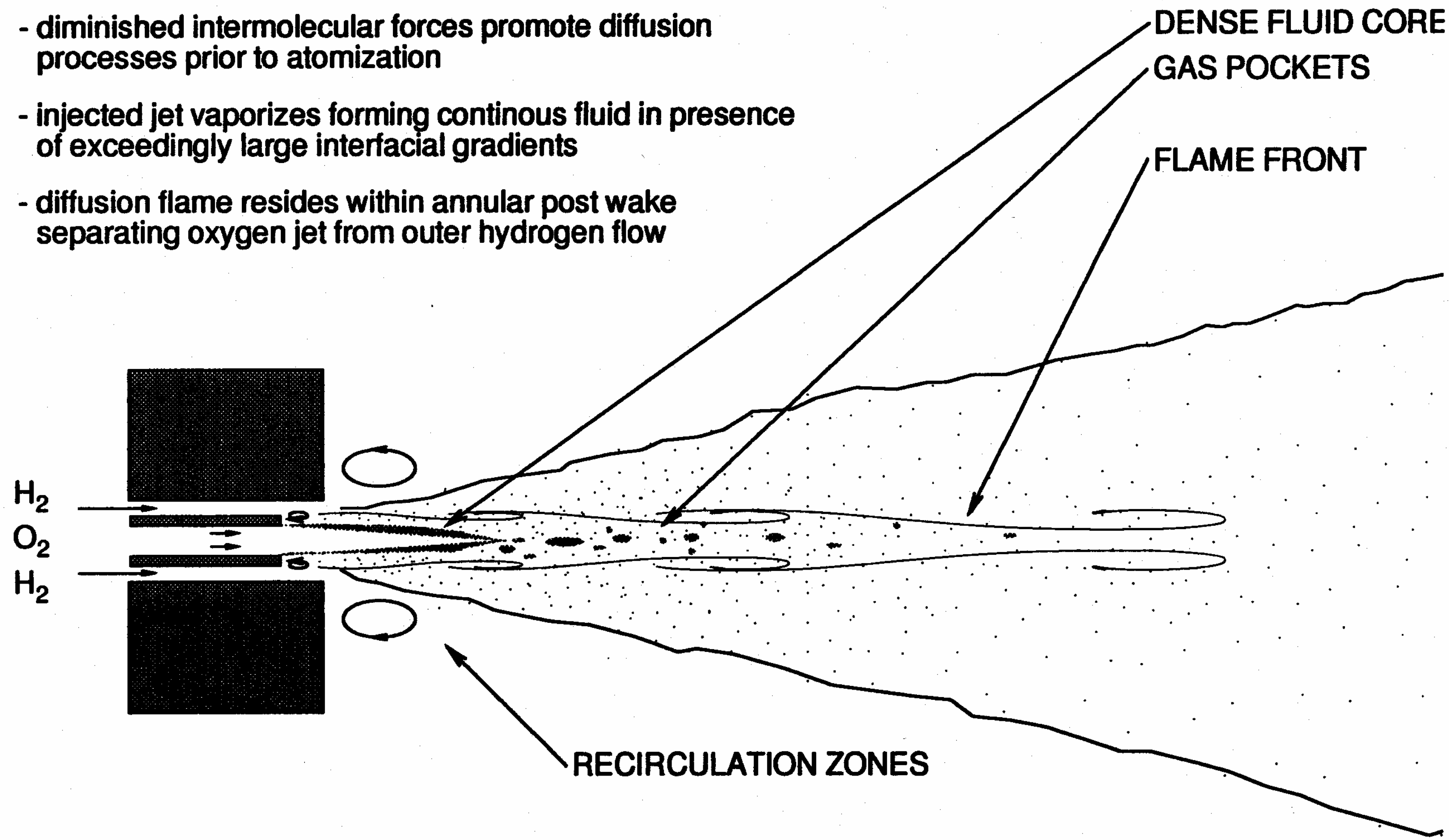

Burning LOX Jet at Supercritical Pressure
(Mayer, DLR, Germany; Tamura, NAL, Japan)

(u_{LOX} = 30 m/s, u_{H_2} = 300 m/s, T_{LOX} = 100 K, T_{H_2} = 300 K, p = 6 MPa)

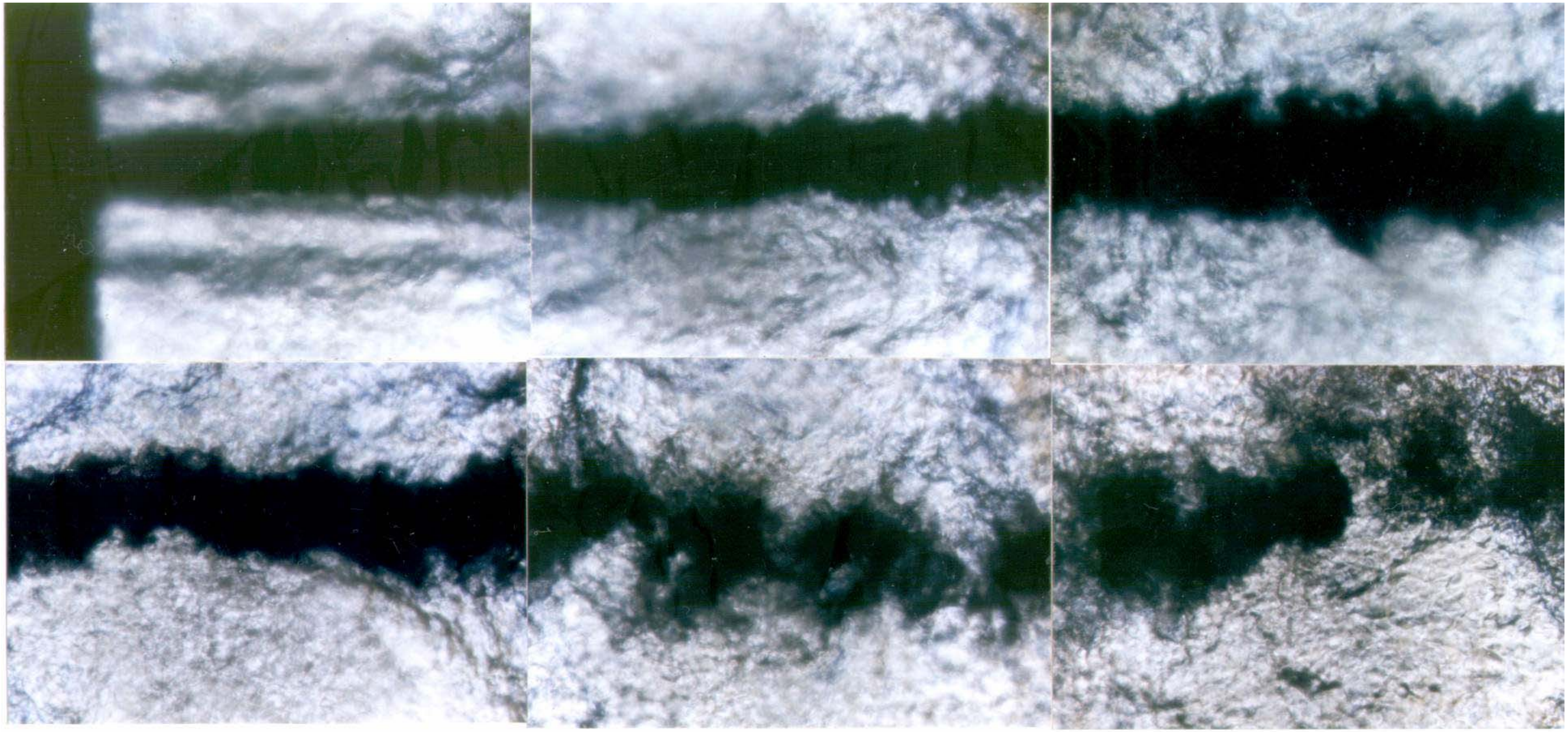

Supercritical Injector Flow and Flame Dynamics

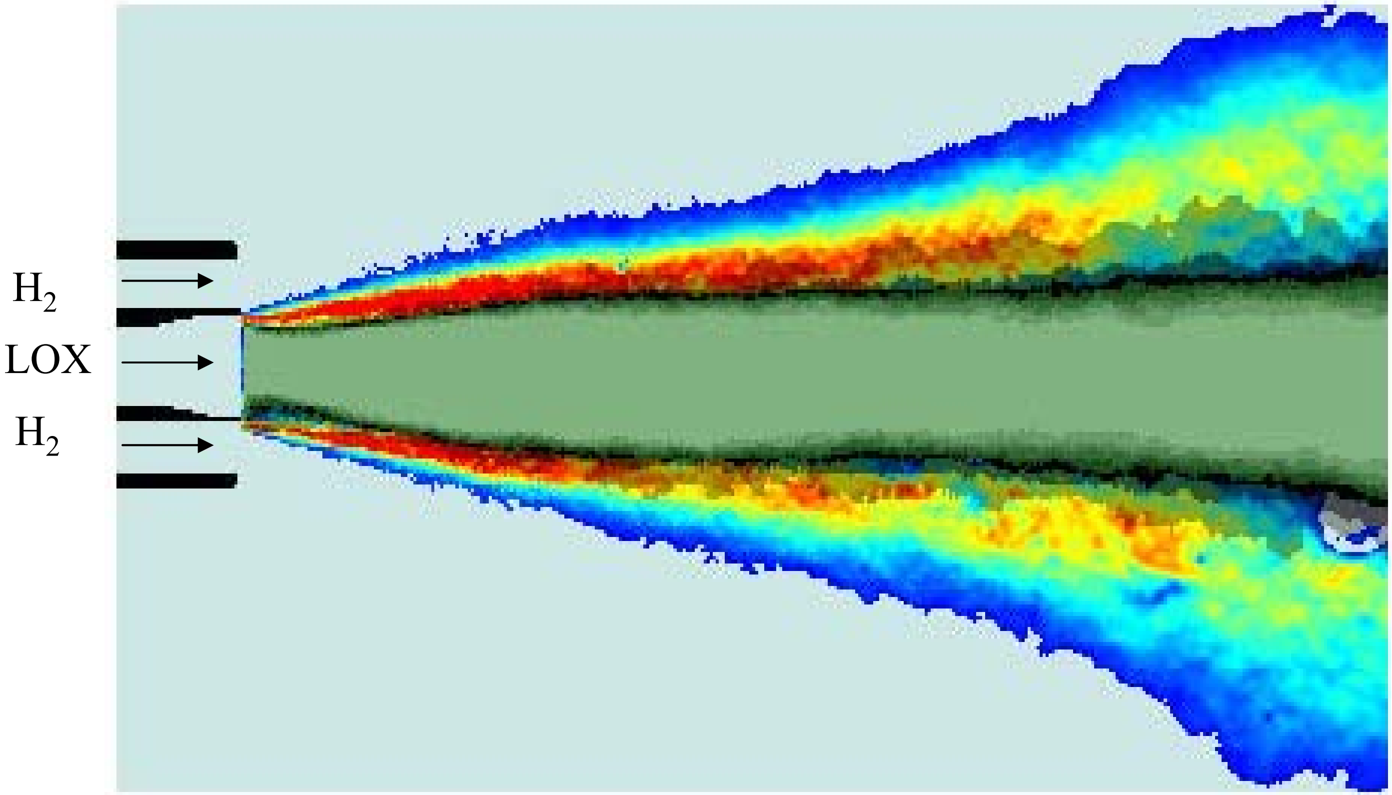

Combined OH emission and backlighting images (Ph.D thesis of Matthew Juniper)

LOX/Hydrogen Shear-Coaxial Injector Dynamics

Department of Mechanical & Nuclear Engineering

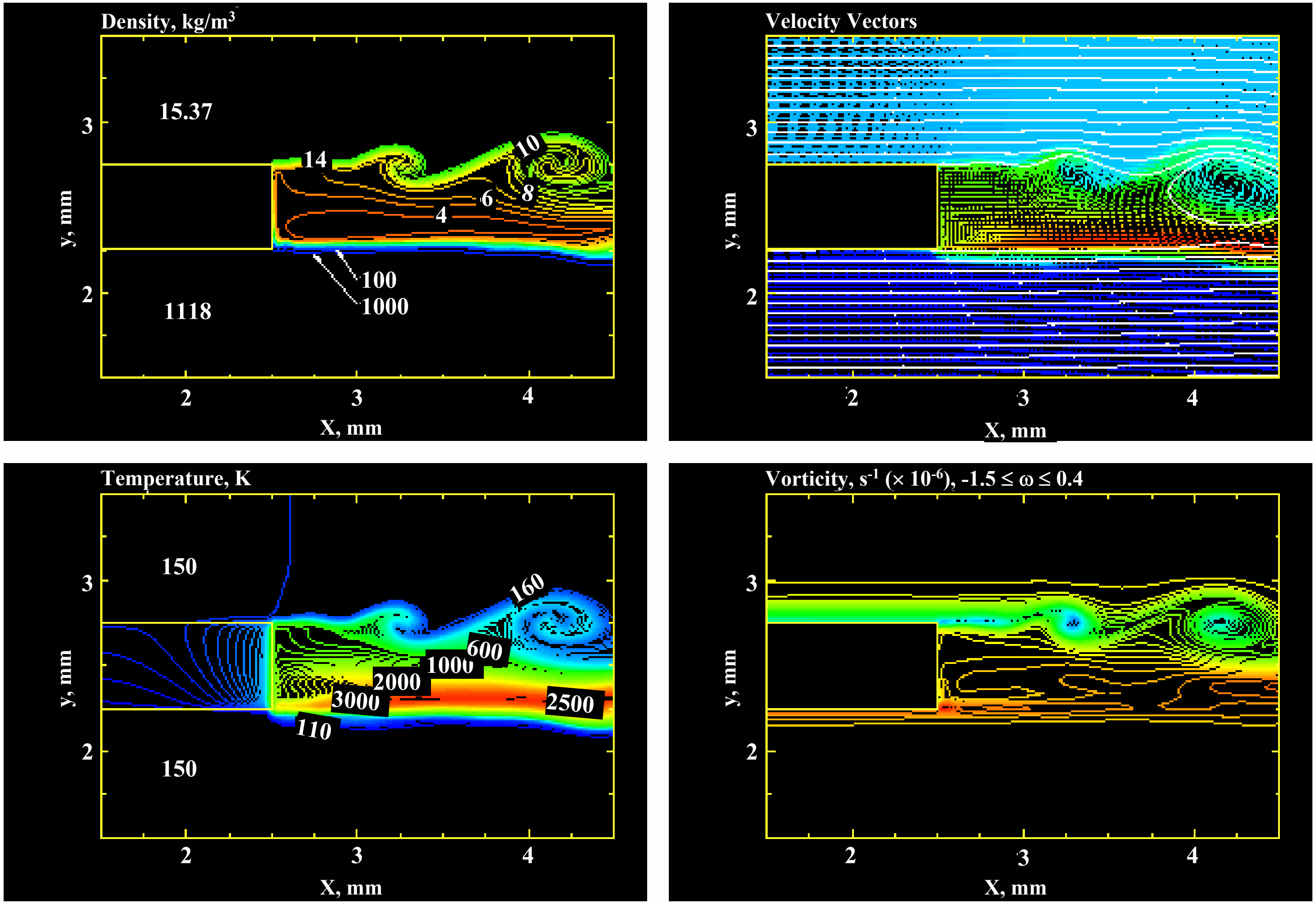

Modeling and Simulation of Supercritical Combustion

Department of Mechanical & Nuclear Engineering

droplet → spray → injector element → full-scale engine

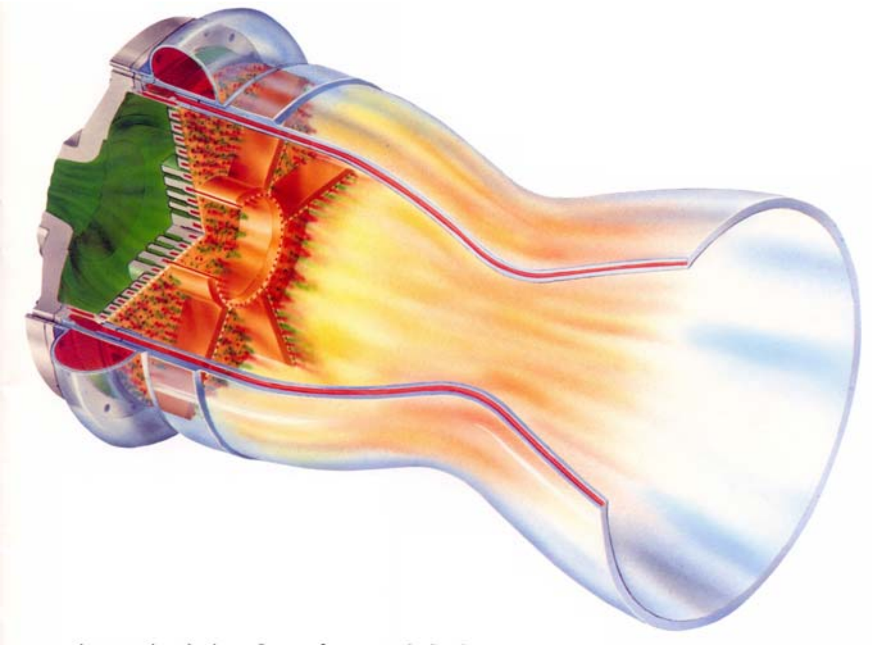

Thank You!

Effect of Pressure on Mean Temperature Distributions

PENNSTATE 1855
Department of Mechanical & Nuclear Engineering

(T_∞ = 300 K, u_{in} = 15 m/s, T_{in} = 120 K, D_{in} = 254 μm)

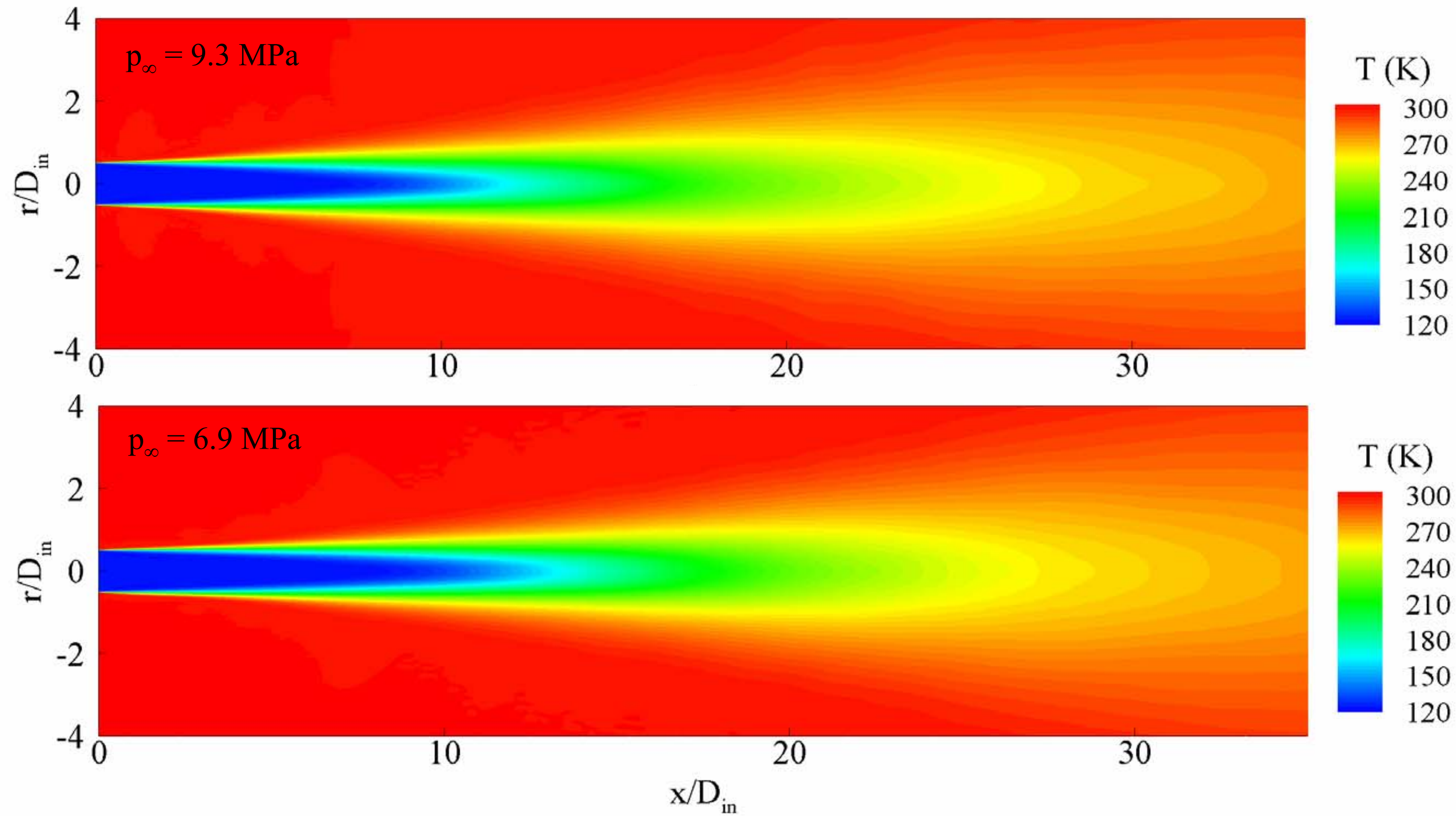

Effect of Pressure on Mean Velocity Distributions

PENNSTATE
1 8 5 5
Department of Mechanical & Nuclear Engineering

(T_∞ = 300 K, u_{in} = 15 m/s, T_{in} = 120 K, D_{in} = 254 µm)

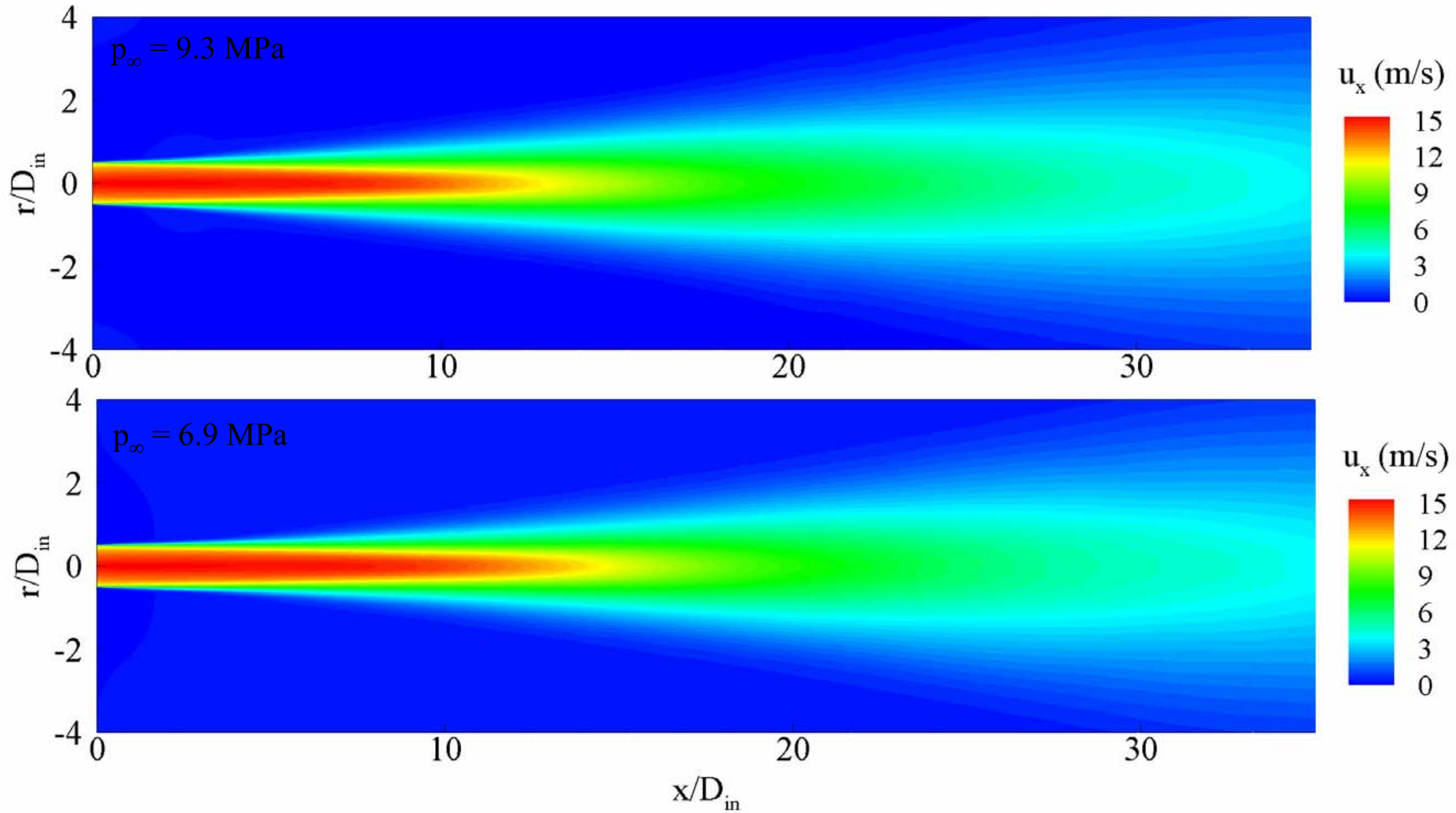

Frequency Spectral of Radial Velocity Oscillations

PENNSTATE
1855
Department of Mechanical & Nuclear Engineering

p = 4.2 MPa | ***p = 6.9 MPa*** | ***p = 9.3 MPa***

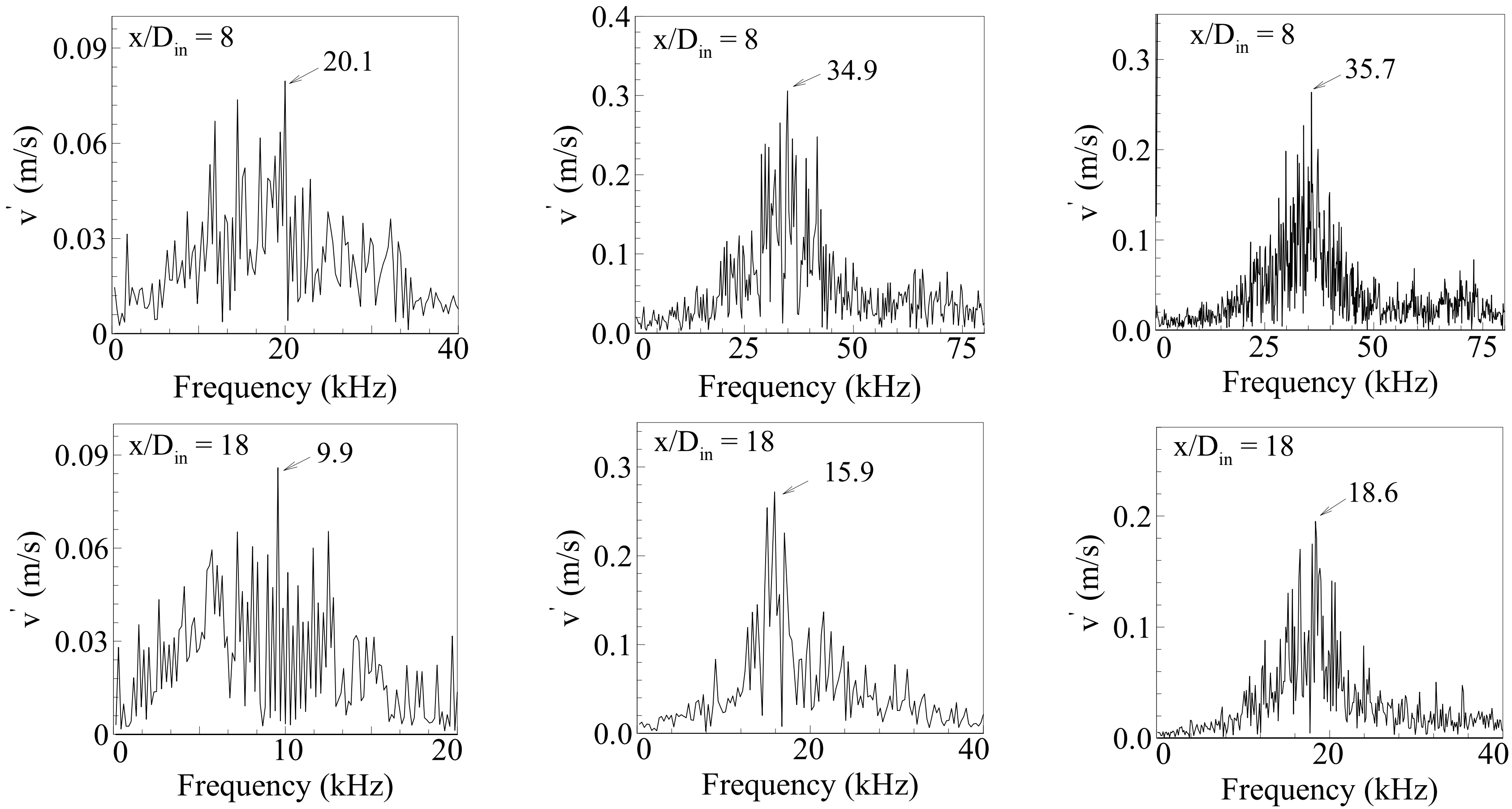

PENNSTATE

Normalized Density and Temperature Distributions along Radial Direction

Department of Mechanical & Nuclear Engineering

T_∞ = 300K, u_{in} = 15m/s, T_{in} = 120K, D_{in} = 254μm)

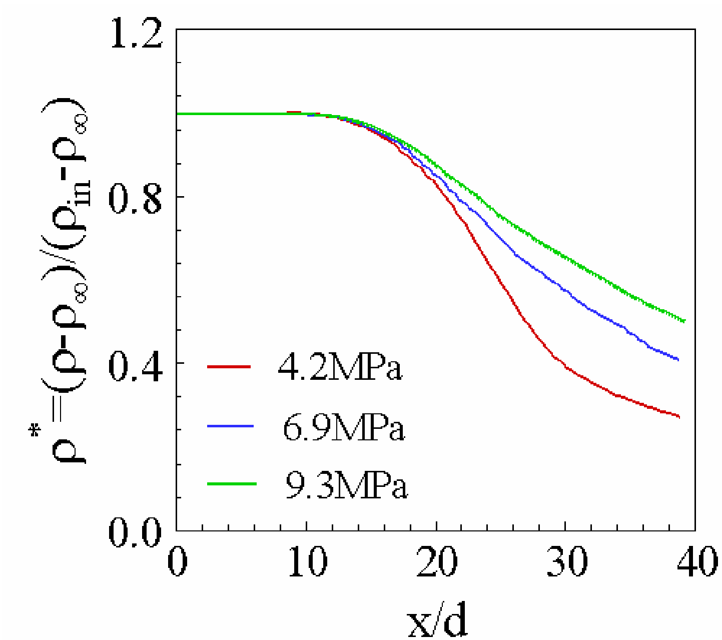

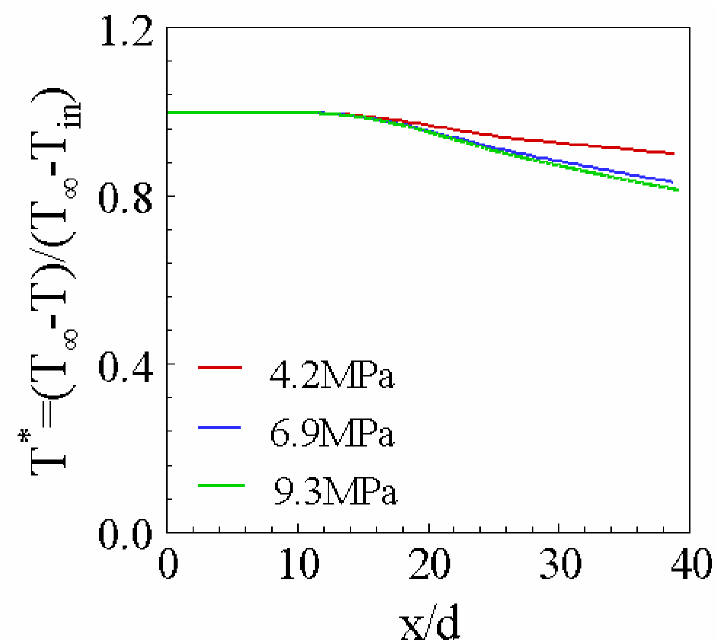

- Thermal diffusivity of nitrogen is relatively lower in the region where the temperature is near the critical temperature.
- Most thermal energy transferred from the hot ambient gaseous nitrogen to the cold jet is used to facilitate volume expansion.

Numerical Challenges

PENNSTATE
1855
Department of Mechanical & Nuclear Engineering

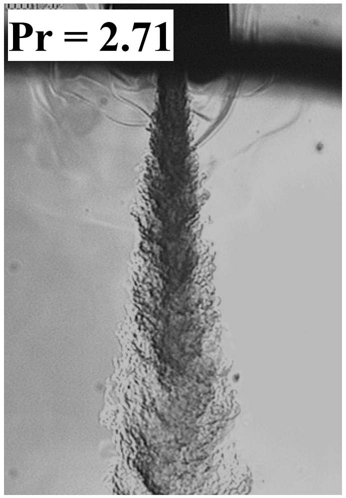

Challenges

- machine round-off errors at low speeds
- eigenvalue disparity
- time accuracy
- real-fluid behavior
- robust and efficient numerical treatment

Solutions

- pressure decomposition
- preconditioning method
- dual time-stepping integration technique
- partial mass/molar properties
- derivation of numerical Jacobians and thermodynamic properties based on fundamental thermodynamic theories

Normalized Density and Temperature Distributions

(p_∞= 9.3MPa, T_∞= 300K, u_{in}= 15m/s, T_{in}= 120K, D_{in}= 254μm)

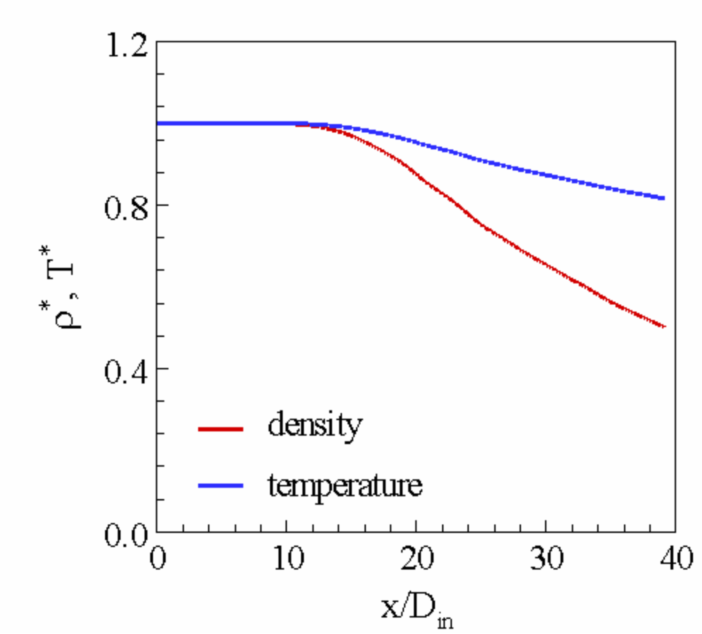

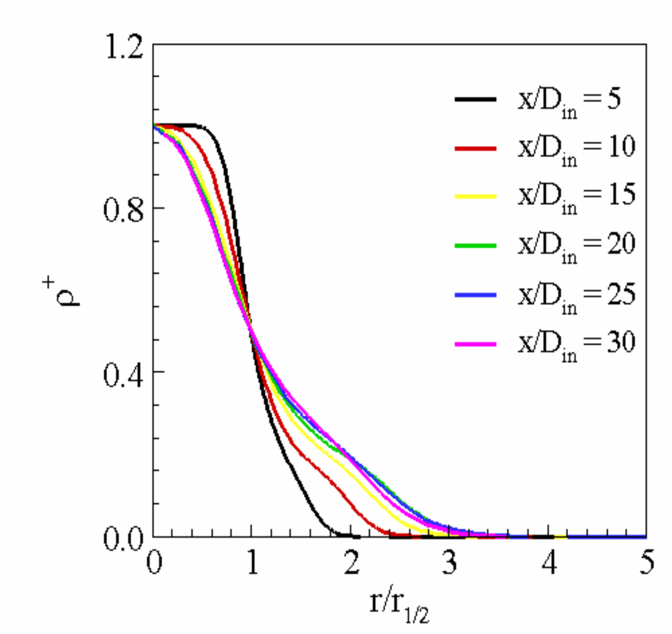

- Due to the "near critical slow down", the temperature of nitrogen fluid increases slowly along the jet centerline.
- A self-similar density profile exist when $x/d > 15$.